

## ABSTRACT

GURARSLAN, ALPER. Single-Component Nylon-6 Composites. (Under the direction of Alan E. Tonelli.)

Polymer composites usually fail at weak interfaces resulting from their chemical incompatibility. The ideal solution to the interface problem would be to make the reinforcing elements from the same polymer as the matrix, called "self-reinforced composites". When producing self-reinforced composite the constituent polymer chains in the fibers must be organized in a way that prevents their complete or even substantial diffusion into the matrix polymer during melt-processing into a single-component composite. Such a reorganization of polymer chains may be achievable by coalescing guest polymers from their crystalline inclusion compounds (ICs) formed with the host cyclodextrins (CDs). Coalesced polymers have recently been observed to be largely extended and unentangled, to crystallize at higher temperatures than their normal entangled melts, and to remain this way even after being held in the melt for considerable periods of time (hours). The same conditions are valid for the films made with the addition of 2wt % of coalesced polymer. Thus, when nucleated polymers are used as the reinforcement fibers and as received polymer is used as the matrix, substantial diffusion of polymer chains from the fiber/matrix into the matrix/fiber is expected to be extremely slow, and should not occur during the times required for composite processing. Furthermore, upon cooling from the melt nucleated film will crystallize before the matrix, and should, for the most part, retain their structural/morphological/ positional integrity and increase the mechanical properties of the composite. Because both components melt during fabrication, at least partially interpenetrated and strong interfaces may be formed causing the fibers to function as effective self-reinforcements in these essentially single-component polymer composites.

Single-Component Nylon-6 Composites

by  
Alper Gurarslan

A thesis submitted to the Graduate Faculty of  
North Carolina State University  
in partial fulfillment of the  
requirements for the Degree of  
Master of Science

Textile Chemistry

Raleigh, North Carolina

2011

APPROVED BY:

---

Dr. Xiangwu Zhang  
Member of Advisory Committee

---

Dr. Michael Dickey  
Member of Advisory Committee

---

Dr. Alan E. Tonelli  
Chair of Advisory Committee

## DEDICATION

This thesis dedicated to my parents for their love and endless support.

## BIOGRAPHY

Alper Gurarslan was born on February 18, 1985 in Sivas, Turkey. He graduated from Usak University, Turkey, department of Textile Engineering with a first honors B.S degree in Textile Engineering in 2007. He started his graduate study at Istanbul Technical University in Polymer Science and Technology Program. In Fall of 2007, he was awarded with two scholarships one from The Scientific and Technological Research Council of Turkey and the other one from Republic of Turkey Ministry of National Education which supports his graduate study in the U.S.A. He attended Intensive English Program in Bloomington, Indiana University. He started his Master study in Textile Chemistry at NCSU, in Fall 2009. He will work as a faculty in Istanbul Technical University after completing his Ph.D. in Fiber and Polymer Science Program at NCSU. He is married to Rana Gurarslan and they have a very beautiful baby girl named Bahar.

## ACKNOWLEDGEMENTS

First and foremost, I would like to thank The Turkish Republic Ministry of National Education for covering my expenses during my language study and master's degree.

I would like to sincerely thank my advisor, Dr. Alan E. Tonelli, for all his guidance and help. The best decision I have ever made was to pursue my graduate research with him.

I would like to thank my committee members Dr. Xiangwu Zhang and Dr. Michael Dickey for their time.

I would like to acknowledge Birgit Andersen, Judy Elson, and Teresa White for teaching me how to use various instruments.

I would like to thank all of my friends who helped me during my research, especially, Abhay Joijode, Huseyin Avci, Ilkay Ozsev Yuksek, and Hicran Koc.

Finally I would like to thank my loving wife, Rana Gurarslan. Without her I couldn't have done any success.

## TABLE OF CONTENTS

<b>Introduction.....</b>	<b>1</b>
<b>Chapter 1. Introduction to Cyclodextrin and Cyclodextrin Inclusion Compounds .....</b>	<b>3</b>
1.1. Introduction.....	3
1.2. Properties of Cyclodextrins .....	4
General Properties .....	4
Crystalline Structures .....	7
1.3. Cyclodextrin Inclusion Complexes .....	9
Reference.....	13
<b>Chapter 2. An Introduction to Self-Reinforced Composites .....</b>	<b>16</b>
2.1 Literature Review .....	16
Reference .....	23
<b>Chapter 3. Producing Single-Component Polymer Composite by Using Coalesced Polymers .....</b>	<b>25</b>
3.1. Introducing a new method to produce single-component polymer composites .....	25
3.2. Experimental .....	28
3.2.1. Materials .....	28
3.2.2. Methods.....	28
3.2.2.1. Inclusion Complex Formation .....	28
3.2.2.2. Coalescence Process .....	29

3.2.2.3. Nucleation Process.....	29
3.2.2.4. Film Production.....	29
3.2.3. Experimental Techniques.....	30
3.2.3.1. Fourier Transform Infrared Spectroscopy.....	30
3.2.3.2. Differential Scanning Calorimeter.....	30
3.2.3.3. Wide Angle X-Ray Diffraction.....	31
3.2.3.4. Tensile Test .....	31
3.2.3.5. Density Measurements.....	33
3.2.3.6. Scanning Electron Microscope.....	33
3.2.3.7. Polarized Optical Microscope .....	34
3.3. Results and Discussion .....	34
3.3.1. Characterization of the Nylon-6- $\alpha$ -Cyclodextrin Inclusion Complex .....	34
3.3.2. Coalescence and Characterization of Nylon 6 .....	38
3.3.3. Employment of Coalesced Nylon-6 as a nucleating agent and Its Characterization .....	42
3.3.4. Single Layer as-r N-6 and nuc N-6 films and their characterization.....	44
3.3.5. Characterization of Single-Component as-r and nuc N-6 Composites .....	53
3.3. Conclusions .....	59
Reference.....	61
<b>Chapter 4. Future Work .....</b>	<b>63</b>
4.1. Future Studies .....	63

## LIST OF TABLES

### **Chapter 1. Introduction to Cyclodextrin and Cyclodextrin Inclusion Compounds**

Table 1. Basic properties of  $\alpha$ -,  $\beta$ -, and  $\gamma$ -cyclodextrin ..... 5

### **Chapter 3. Producing Single-Component Polymer Composite by Using Coalesced Polymers**

Table 1. Nylon-6 Densities ..... 42

Table 2. Tensile test results for single layer as-r and nuc N-6 films..... 47

Table 3. Crystallinity values of as-r, nuc, and annealed N-6 single layer films ..... 51

## LIST OF FIGURES

### Chapter 1. Introduction to Cyclodextrin and Cyclodextrin Inclusion Compounds

Figure 1. Number of cyclodextrin publications over the past 120 years .....	3
Figure 2. Chemical structure and numbering of $\alpha$ -, $\beta$ -, and $\gamma$ -cyclodextrin .....	5
Figure 3. Location of the hydrophobic and hydrophilic interactions for cyclodextrin .....	6
Figure 4. Glucopyranose unit .....	7
Figure 5. The Herringbone (A) and Layer (B) cage structures, and head to head:tail to tail (C) and head to head-tail to head:tail to tail (D) Channel crystal structures.....	8
Figure 6. X-Ray diffraction for as received $\alpha$ -CD and Nylon-6 $\alpha$ -CD IC .....	9
Figure 7. Schematic representation of polymer cyclodextrin complex formation .....	10
Figure 8. Schematic representation of non-stoichiometric polymer-cyclodextrin IC formation.....	11
Figure 9. Schematic representation of the coalescence process.....	12

### Chapter 2. An Introduction to Self-Reinforced Composites

Figure 1. Diagram of preparing single polymer composite by the partial melting method .....	20
Figure 2. Plain N-6 cloth and cross-section morphology of plain N-6 cloth partially melted at 226 °C. ....	21

### Chapter 3. Producing Single-Component Polymer Composite by Using Coalesced Polymers

Figure 1. Flow diagram of this study.....	27
Figure 2. Picture of a dumbbell specimen for tensile test .....	32
Figure 3. FTIR scans for $\alpha$ -CD, 1:1 N-6 $\alpha$ -CD-IC, and bulk N-6.....	35
Figure 4. DSC heating scans for as-r N-6, 1:1 N-6 $\alpha$ -CD-IC .....	36
Figure 5. WAXD of cage crystalline structure of pure $\alpha$ -CD and columnar crystalline structure of N-6- $\alpha$ -CD-IC .....	37
Figure 6. FTIR scans of $\alpha$ -CD, 1:1 N-6 of $\alpha$ -CD IC, as-r N-6, and coalesced N-6 .....	38
Figure 7. DSC heating and cooling scans for coalesced N-6.....	40
Figure 8. Parallel ( $\gamma$ ) and anti-parallel ( $\alpha$ ) N-6 chains .....	40

Figure 9: WAXD scans for as-r and coalesced N-6 ..... 41

Figure 10. DSC scans of N-6 and nuc N-6 ..... 43

Figure 11. Polarized Optical Microscope images for melt crystallized films of neat N-6 and nuc N-6 44

Figure 12. DSC of single layer as-r N-6 film and single layer nuc N-6 film ..... 45

Figure 13. Response of single layer as-r (upper) and nuc (lower) N-6 films to applied load ..... 46

Figure 14. Load-strain curves of single layer as-r N-6 and nuc N-6 ..... 49

Figure 15. Energy associated with increments of strain ..... 50

Figure 16. Stress-strain responses of thin melt-pressed neat bulk N-6 films (as-received and annealed), and N-6 film nucleated with N-6 coalesced from its 1:1 stoichiometric  $\alpha$ -CD-IC ..... 52

Figure 17. Schematic representation of two layer as-r N-6 sandwich, and Single - Component as-r N-6/nuc N-6 Composite ..... 53

Figure 18. DSC cooling scans from the melts of (I) as-received , (II) nucleated, and (III) asr/nuc sandwich films..... 55

Figure 19. Tensile tests results for asr/asr and asr/nuc N-6 sandwich films ..... 57

Figure 20. Response of asr/asr (left) and asr/nuc (right) N-6 sandwich film to applied load ..... 58

Figure 21. SEM images of the cross section of single-component as-r/nul-N-6 composite ..... 59

## INTRODUCTION

There is strong correlation between the properties of polymer materials and their solid state morphologies. It is possible to obtain desired properties by manipulating a polymer's morphology, which is possible by controlling its processing. In this study, we are processing polymers with cyclodextrin at the industrial macromolecular level and obtain distinct and improved properties in comparison to bulk polymers processed from their solutions and melts.

Cyclodextrins are cyclic starch molecules composed of  $\alpha$ -1,4-linked glucose units. Most widely used are alpha, beta, and gamma cyclodextrins which have 6, 7, and 8 glucose units, respectively. These cyclically attached glucose units form a hydrophobic internal cavity and a hydrophilic outer surface. Depending on their cavity size, it is possible to include a variety of molecules and polymer chains inside their cavities and form non-covalently bonded inclusion compounds (ICs), and are widely used in the pharmaceutical industry. The first polymer-cyclodextrin inclusion compound was obtained by Harada and Kamachi using poly(ethylene oxide) oligomers and  $\alpha$ -cyclodextrin in 1990. Subsequently, his threading technique was applied on numerous polymers.

However, for some applications it is more convenient to remove the cyclodextrin and use the polymers coalesced from their ICs. These coalesced polymers are significantly different from normally processed polymers. Polymer chains included in their cyclodextrin channels are highly extended and un-entangled, and they largely retain these characteristics even after removing the cyclodextrin.

After the coalescence process, crystallizable polymers exhibit higher melting, crystallization, and decomposition temperatures, while amorphous polymers exhibit higher glass-transition temperatures,  $T_g$ , than samples obtained from their solutions and melts. Moreover coalesced polymers retain these altered specific properties even after holding them in the melt or above  $T_g$  for long times. This means that they will retain their as-coalesced morphologies after normal thermal processing conditions. Furthermore, when these coalesced polymers are used in small amounts, they can successfully nucleate the crystallization of the same as-received polymers, which then show the same enhanced crystallizabilities, because upon cooling from the melt, coalesced polymers crystallize before bulk polymers.

Because of their thermal stability, nucleated polymers do not rapidly mix with as-received polymers. As a result, it is possible to produce a self-reinforced composite by using nucleated polymers as reinforcement and bulk as-received polymers as matrix *via* melt processing. During melt processing, these two components can partially interpenetrate and interlock with each other, yielding a good adhesion between the interfaces, but without losing their individual characteristics, and resulting in improved mechanical properties.

# CHAPTER 1

## Introduction to Cyclodextrin and Cyclodextrin Inclusion

### Compounds

#### 1.1 Introduction

In 1891 A. Villears first discovered cyclodextrins (CDs) and named them cellulosine [1]. There have been numerous researches conducted on cyclodextrins since 1891 and Figure 1 schematizes the cumulative CD publications. As seen there, studies on CDs can be divided into three main parts: Discovery of their Structures, Chemical and Inclusion Properties, and Industrial Production of Cyclodextrins.

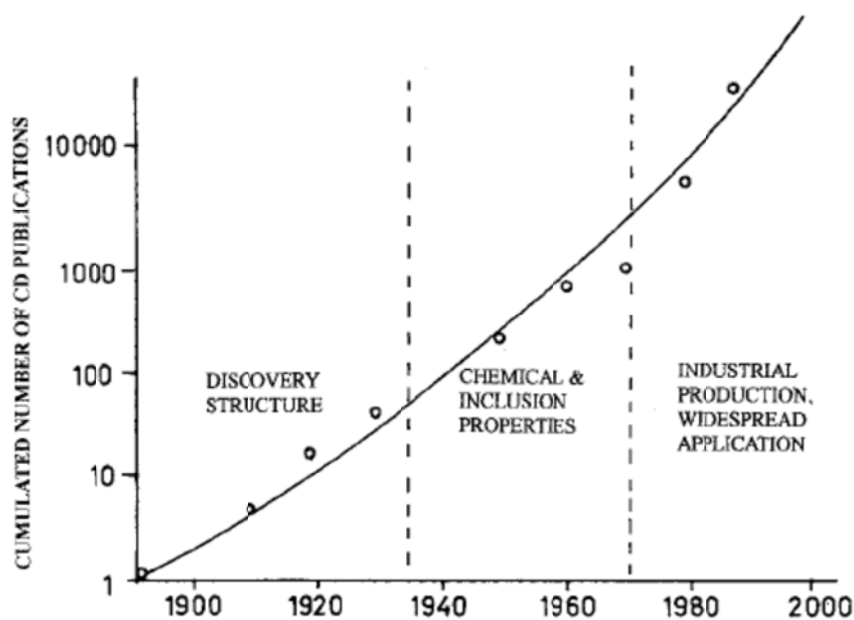


Figure 1. Number of cyclodextrin publications over the past 120 years [2].

Although Villears discovered the cyclodextrins, Schardinger was the first scientist to name these cyclic-oligosaccharides. He also distinguished  $\alpha$ - and  $\beta$ -cyclodextrins, relying on the color of an iodine complexation [3].

In the 1930's Freudenberg and Jacobi discovered  $\gamma$  cyclodextrin and they showed that these cyclic starch molecules are composed of  $\alpha$ -1,4-linked glucose units [4]. Until the 1970's structural, chemical, and physiochemical characteristics of cyclodextrins were studied extensively by Cramer [5], and after the 1970's, industrial production of cyclodextrins increased dramatically because they started to be used in various applications.

In the last decade, cyclodextrins were employed mostly in pharmaceutical applications. CD complexation of drug molecules allows release of drugs in a controlled fashion through control of the solubility of drug molecules [6]. Cyclodextrins provide new production and processing techniques. More interestingly, they can be used as an effective tool to improve our knowledge of polymer physics [7].

## **1.2 Properties of Cyclodextrins**

### **1.2.1 General Properties**

Cyclodextrins are cyclic starch molecules composed of  $\alpha$ -1,4-linked glucose units. Cyclodextrins can be produced by a simple enzymatic conversion of starch, which is an environmentally friendly and cheap procedure [2]. Most widely used cyclodextrins are alpha, beta, and gamma cyclodextrins which have 6, 7, and 8 d-glucose units, respectively. Figure 2

shows the cyclic structure of cyclodextrins, and some of their basic properties are listed in Table 1.

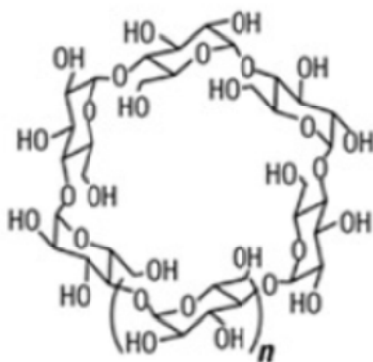


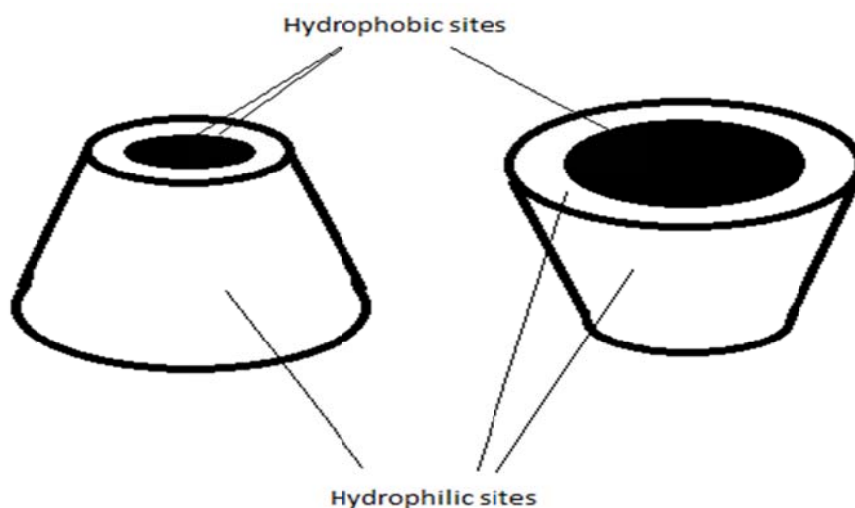
Figure 2. Chemical structure and numbering of  $\alpha$ -,  $\beta$ -, and  $\gamma$ -cyclodextrin ( $n=1$  for  $\alpha$ ,  $n=2$  for  $\beta$ , and  $n=3$  for  $\gamma$ ) [8].

Table 1: Basic properties of  $\alpha$ -,  $\beta$ -, and  $\gamma$ -cyclodextrin [8].

Property	$\alpha$ -CD	$\beta$ -CD	$\gamma$ -CD
Number of glucopyranose units	6	7	8
Molecular weight (g/mol)	972	1135	1297
Solubility(% w/v in water, 25 °C)	14.5	1.85	23.2
Outer diameter (Å)	14.6	15.4	17.5
Cavity diameter (Å)	4.7-5.3	6.0-6.5	7.5-8.3
Cavity depth (Å)	7.9	7.9	7.9
Cavity volume (Å <sup>3</sup> )	174	262	427

\*Values vary slightly depending on source

The most important structural characteristics of cyclodextrins are their cylindrical shape and the hydrophilic hydroxyl groups on the outer surface. Cyclodextrins are not exactly cylindrical molecules, but to some extent are truncated cones. Their glucopyranose units cause this conic shape, because they hinder bond rotation. All the primary hydroxyl groups are located on their narrow rim, while all the secondary hydroxyl groups are located on the wider rim of the cyclodextrins [9]. The aliphatic ring hydrogen atoms are directed inwards, as are the glycosidic oxygen bridges that connect the glucopyranose rings [8]. This conformation creates a lipophilic cavity and a hydrophilic outer surface, as depicted in Figure 3. Having both hydrophilic and lipophilic properties, place cyclodextrins in a special position as drug delivery systems [9].



**Figure 3. Location of the hydrophobic and hydrophilic interactions for cyclodextrin [3].**

The hydrophilic outer surface of cyclodextrins makes them soluble in hydrophilic-compatible solvents, such as water and DMSO. As seen in Table 1,  $\beta$ -CD has much lower solubility in water than  $\alpha$ - and  $\gamma$ -CD's. [10]. According to molecular dynamic computer

simulations,  $\beta$ -cyclodextrin has highly dense local water structure both inside and outside its cavity, as seen in Figure 4. These surrounding water molecules, decreases the internal motions of  $\beta$ -cyclodextrin and creates a more rigid cyclic structure than  $\alpha$ - and  $\gamma$ -cyclodextrins. Surrounding water molecules and a relatively rigid assembly of  $\beta$  cyclodextrin decreases the configurational entropy, which yields much lower water solubility for  $\beta$ -cyclodextrin.

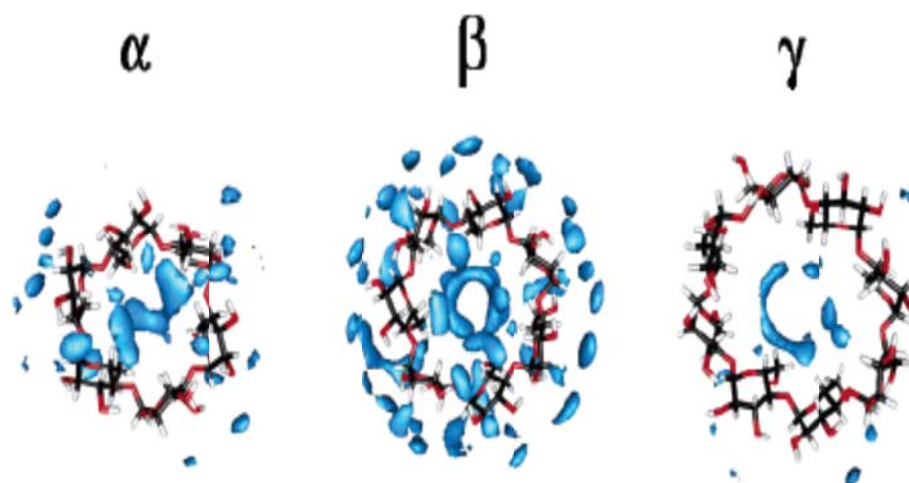


**Figure 4. Molecular Dynamic computer simulation depicts local water molecules around the cyclodextrins. [10]**

### **1.2.2 Crystalline Structures**

Cyclodextrins may adopt four kinds of crystalline structures, which can be placed in 2 main classes. One class is cage crystalline structures, which are generally formed by pure cyclodextrins or their ICs containing small guests. The second type is columnar structures, where the cavities of cyclodextrins are parallel to each other. In order to have such a columnar structure

there usually must be some long guest, like polymeric chains, included inside the cyclodextrin cavities. Figure 5 depicts the cage and columnar crystalline structures.

The crystalline structures of cyclodextrins can be differentiated by wide angle X-ray diffraction (WAXD). The WAXD pattern for as received  $\alpha$ -CD and its inclusion complex with Nylon-6 can be seen in Figure 6. From this figure it is clear that CDs shift their crystalline structure from cage to columnar form when we include some guest polymer chains inside their cavities.

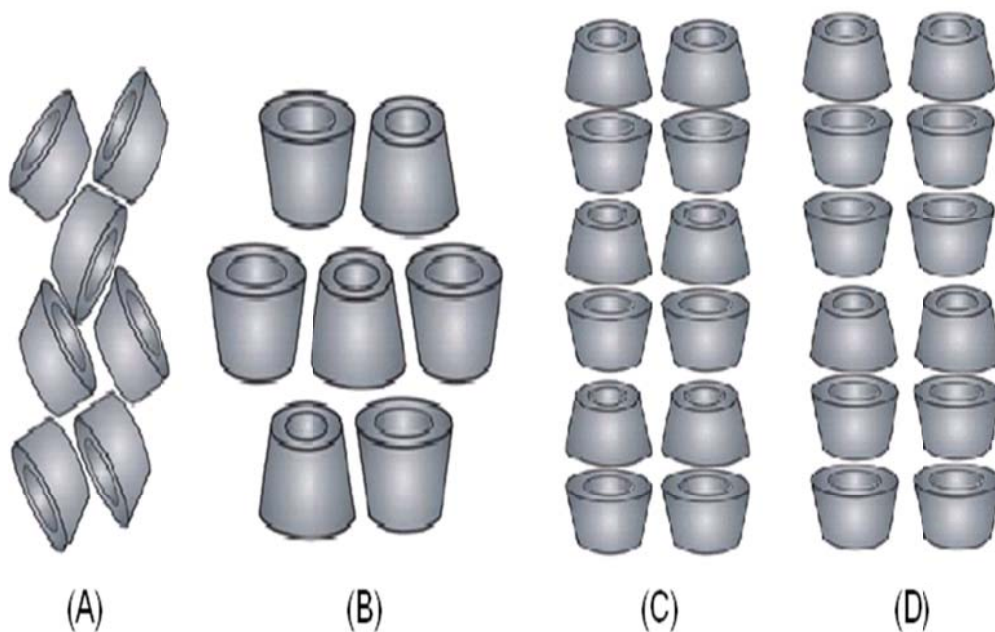


**Figure 5. The Herringbone (A) and Layer (B) cage structures, and head to head-tail to tail (C) and head to head-tail to head-tail to tail (D) Channel crystal structures [8].**

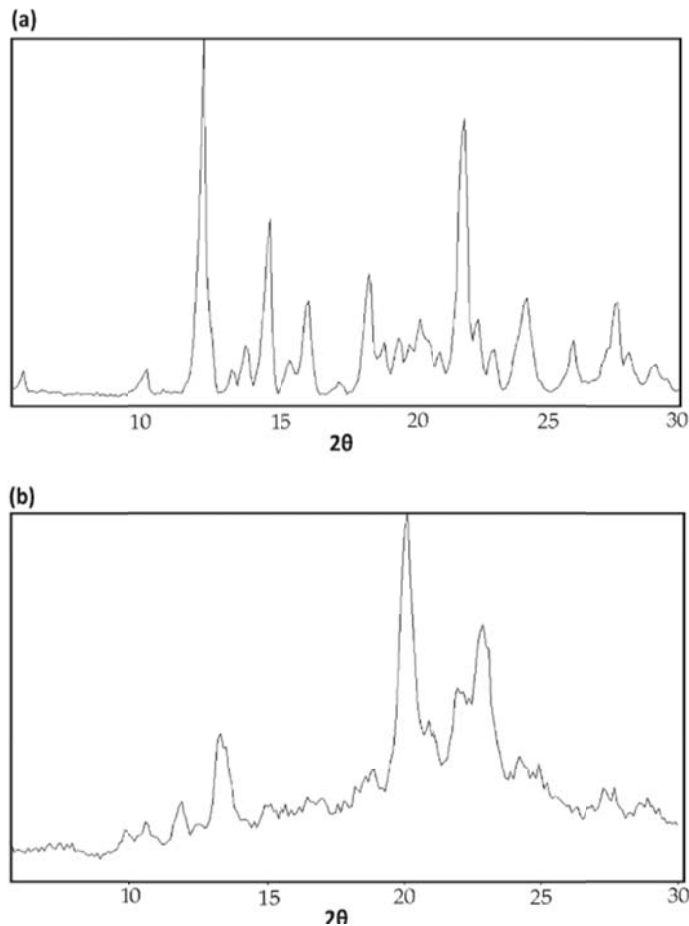


**Figure 6. X-Ray diffraction for (a) as received  $\alpha$ -CD and (b) Nylon-6-  $\alpha$ -CD IC [11].**

### 1.3. Cyclodextrin Inclusion Complexes

As explained previously, cyclodextrins have hydrophilic outer surfaces and hydrophobic cavities. When cyclodextrins contact hydrophobic molecules, they prefer to stay inside the cavity of cyclodextrin and form a new complex material, called an inclusion complex. Although there are no covalent bonds between the guest molecule and the host cyclodextrin cavity, they stay together. Ions [12], small molecules [13], monomers [14], dyes [15], oligomers, and polymers [16-19] can be complexed inside cyclodextrin cavities.

Harada and Kamachi first reported inclusion complexes formed between CDs and poly (ethylene glycol) (PEG) [20] in 1990, and thereafter, Harada et al and Tonelli et al [21] have conducted extensive studies on polymer-cyclodextrin inclusion compounds. Figure 7 schematizes complex formation between guest polymer chains and cyclodextrins.

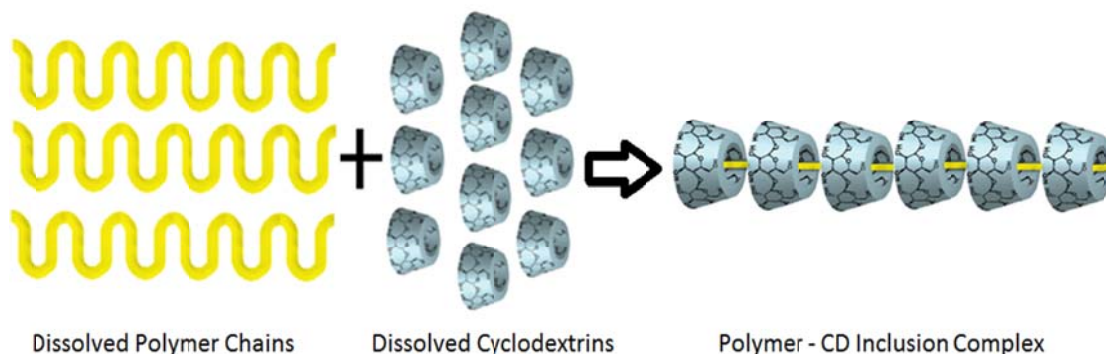


**Figure 7. Schematic representation of polymer cyclodextrin complex formation**

Formation of polymer-cyclodextrin ICs depends on the type of cyclodextrin, the polymer and its molecular weight, solvent and temperature [21]. The inclusion process represented in Figure 7 was modeled by Baglioni et al to occur in five main steps [22].

1. Diffusion of polymer chains and CD molecules
2. Threading of polymer chain ends into the CD cavities
3. Movement of CD molecules through the polymer chains
4. De-threading of CD molecules off of the polymer chains
5. Precipitation of the final aggregate

Mohan (in her PhD thesis) and others before her showed that it is possible to make non-stoichiometric inclusion compounds by using excess polymer [23]. In this case, since the amount of cyclodextrin is not enough to cover the entire guest polymer chains, only partial coverage occurs. Formation of non-stoichiometric Polymer-CD-IC can be seen in Figure 8.

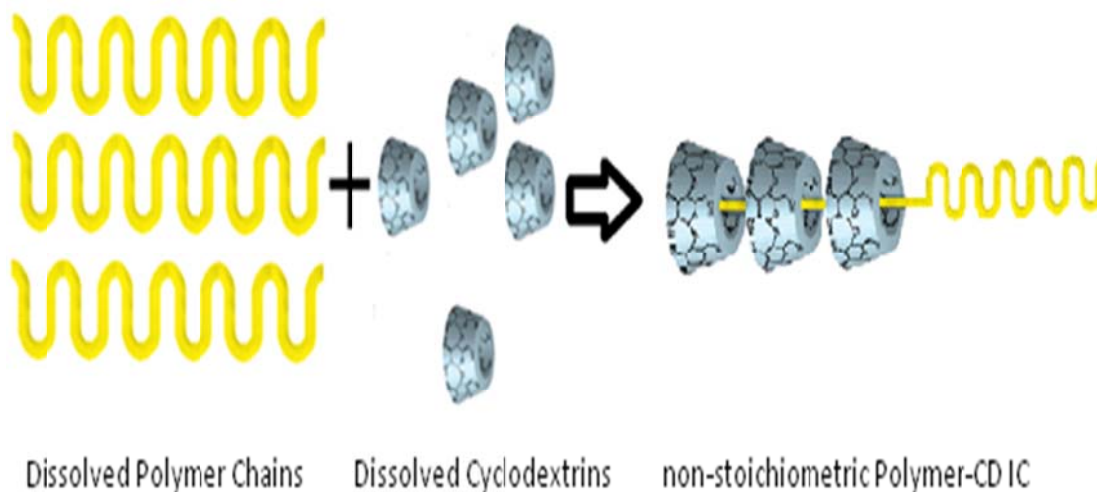


**Figure 8. Schematic representation of non-stoichiometric Polymer-CD IC formation**

There is an interesting process called coalescence, which occurs after carefully removing the host cyclodextrin. The guest polymer chains coalesce to form a bulk solid sample with an arrangement of chains distinct from that normally produced from their randomly-coiling and entangled solutions or melts (See Figure 9). This expectation has indeed been confirmed numerous times in studies of Tonelli et al [7].

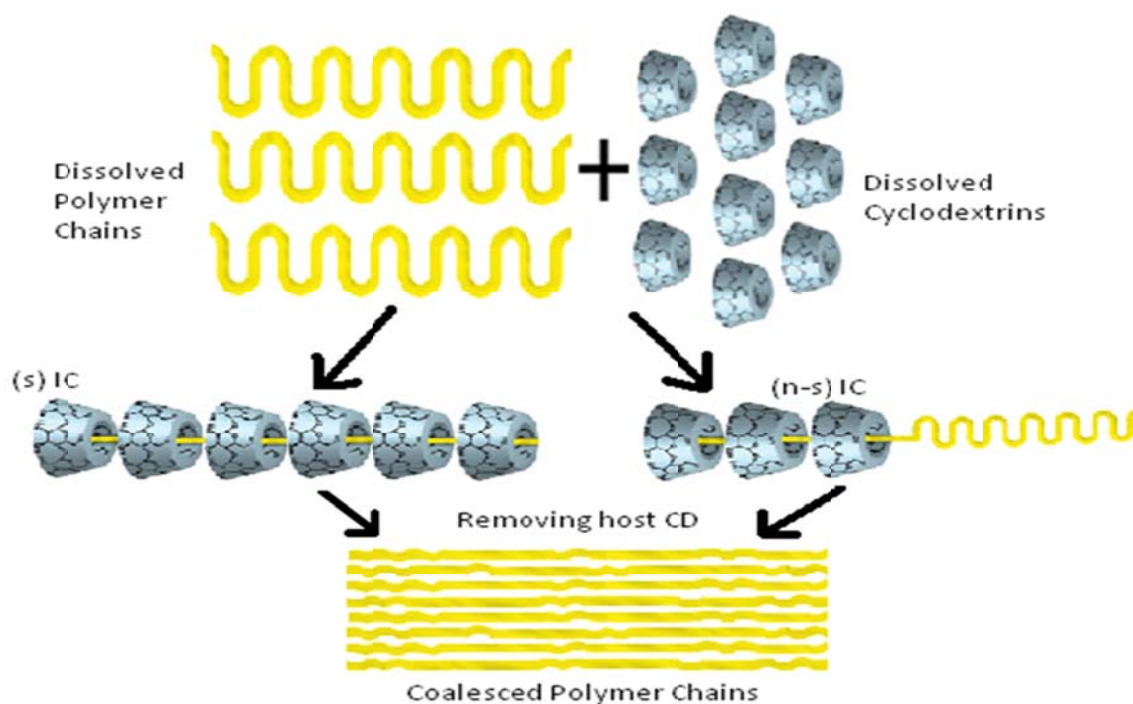


**Figure 9. Schematic representation of the coalescence process.**

Coalesced polymers, as depicted in Figure 9, have a new organization, which may lead to distinct properties. In fact, observations show that upon coalescence from their CD-ICs; i.) crystallizable polymers evidence increased levels of crystallinity, unusual polymorphs, and higher melting ( $T_m$ ), crystallization, and decomposition temperatures, while coalesced amorphous homopolymers exhibit higher glass-transition temperatures ( $T_g$ ) than samples consolidated from their disordered solutions and melts; ii.) molecularly mixed, intimate blends of two or more polymers that are normally believed immiscible can be obtained upon coalescence from their common CD-ICs, iii.) the phase segregation of incompatible blocks can be controlled (either suppressed or enhanced) in coalesced block copolymers, and, most importantly, iv.) the thermal and temporal stabilities of the organization of coalesced neat

homopolymers, well-mixed homopolymer blends, and block copolymers are substantial, thereby suggesting retention of their as-coalesced structures and morphologies under normal thermal processing conditions. Observation iv.) has recently been suggested to be the result of the long times necessary for the many chains influenced by a single coalesced polymer chain, after it is randomly-coiled, to establish a fully entangled melt [24].

## REFERENCES

1. Villiers A. On the fermentation of starch by the action of the ferment butyric, Comptes Rendus de l'Académie des, Vol. 112, pp. 536-538. 1891.
2. Szejtli, J. Chem. Rev. 98, 1743-1754. 1998.
3. Schardinger F, Zentralblatt B. 2, 29, 188. 1911.
4. Freudenberg K, Meyer-Delius M. Ber. Dtsch. Chem. Ges, 2, 71, 1596-1600. 1938.
5. Cramer F. Inclusion Compounds. Berlin : Springer-Verlag, 1954.
6. Uekama K, Hirayama F, Irie T. Cyclodextrin Drug Carrier Systems, Chem. Rev.98  
2045-2076. 1998.
7. Tonelli AE. Molecular Processing of Polymers with Cyclodextrins, Adv Polym Sci, 222: 115–  
173. 2009.
8. Williamson BR. Processing Polymers with Cyclodextrins. PhD Thesis. North Carolina State  
University. 2010.
9. El-Nokaly MA, David MP, Charpentier BA. Polymeric Delivery Systems. Washington , DC:  
American Chemical Society. 1993.
10. Naidoo JK, Chem JYJ, Janson JLM, Widmalm G, Maliniak Arnold. J. Phys. Chem. B. 108,  
4236. 2004.

11. Mohan A, Joyner X, Kotek R, Tonelli AE. The Constrained/Directed Crystallization of Nylon-6:1. Non-stoichiometric Inclusion Compounds formed with Cyclodextrins, *Macromolecules*, 42, 8983-8991. 2009.
12. Bajpai M, Gupta P, Bajpai SK. Silver(I) Ions Loaded Cyclodextrin-Grafted-Cotton Fabric with Excellent Antimicrobial Property, *Fibers and Polymers*, 11, 1, 8-13. 2009.
13. Rusa CC, Bridges C, Ha S, Tonelli AE. *Macromolecules*, 38, 5640-5646. 2005.
14. Uyar T, El-Shafei A, Wang X, Hacaloglu J, Tonelli AE. *J. Incl. Phenom. Macro*, 55, 109-121. 2006.
15. Suzuki M, Tsutsui M, Ohmori H. *Carbohydr Res*, 261, 223-230. 1990.
16. Rusa C, Rusa M, Peet J, Uyar T, Fox J, Hunt M, Wang X, Balik C, Tonelli AE. *J. Incl. Phenom. Macro*. 55, 185-192. 2006.
17. Wei M, Tonelli AE. *Macromolecules* 34, 4061-4065. 2001.
18. Martínez, G, Gómez MA, Villar-Rodil S, Garrido L, Tonelli AE, Balik CM. *J. Polym. Sci. Pol. Chem.* 45, 2503-2513. 2007.
19. Rusa CC, Shuai X, Shin ID, Bullions TA, Wei M, Porbeni FE, Lu J, Huang L, Fox J, Tonelli AE. *J. Polym. Environ.* 12, 157-163. 2004.
20. Harada A, Kamachi M. Complex formation between poly(ethylene glycol) and alpha-cyclodextrin, *Macromolecules*, Vol. 23 10. 1990.

21. Rusa CC, Rusa M, Peet J, Uyar T, Fox J, Hunt MA, Wang X, Balik CM, Tonelli AE, The Nano-threading of Polymers, *J. Inclus. Phenom. & Macrocyc. Chem.*, 55,185, 2006.
22. Becheri A, Lo Nostro P, Ninham BW, Baglioni P. *J. Phys. Chem. B* 107, 3979-3987. 2003.
23. Mohan A. Modification of Nylon 6 Structure via Inclusion. PhD Thesis. North Carolina State University. 2009.
24. Tonelli AE. Organizational Stabilities of Bulk Neat and Well-Mixed, Blended Polymer Samples Coalesced from Their Crystalline Inclusion Compounds Formed with Cyclodextrins, *J. Polym. Sci.Part B, Polym.Phys. Ed.*, 47, 1543, 2009.

## CHAPTER 2

### An Introduction to Self-Reinforced Composites

#### 2.1. Literature Review

There is no universally accepted definition for a composite material. For some optimistic researchers materials composed of two or more identifiable constituents are composites, and not homogenous or single phase materials. On the other hand, there is another group who think composite materials do not include sandwiches, laminates, felts, etc., but consist only of reinforcing phase structures embedded in a continuous matrix phase. In his book, Lee defines composite materials as “a multiphase material formed from a combination of materials which differ in composition or form, remain bonded together, and retain their identities and properties” [1]. Since this appears to be a comprehensive and judicious definition, we are going to adopt it here.

In many cases, a strong and stiff component is embedded in a softer constituent component forming the matrix [2]. For instance, bone and teeth are both essentially composed of hard inorganic crystals (hydroxyapatite or osteons) in a matrix of tough organic constituents called collagen [3].

A composite material possesses properties that are improved compared to those of its components [1]. In fact, this feature of composites provides them with broad areas of applications, such as from aerospace to automotive; and architecture to agriculture [2].

Composites are very important engineering materials, because it is possible to tune the desired properties of final products by manipulating the volume fractions of the matrix and the reinforcement. Although the volume fraction of reinforcement has profound impact on final properties, interactions at the interfaces between composite components are the defining/limiting feature of composite behavior. If there is poor adhesion between components at their interfaces, composites break when the weaker component breaks. Unfortunately, polymer-polymer composites usually fail due to the poor adhesion at the interfaces resulting from their chemical incompatibility.

Researchers have been trying to improve adhesion between the fiber and the matrix in different ways. Grafting of polymer chains has been proposed as a means to improve adhesion. For instance, Mobarakeh et. al. covalently grafted Nylon 6,6 onto Kevlar fibers to maximize the interface diffusion between the matrix and the dangling polymer chains attached to the Kevlar fiber. They report increase in strength and modulus of composites even at the low fiber percentage used [4]. When a similar approach was applied on polystyrene-Kevlar composites, polymerization of styrene onto Kevlar fibers led to an increase of up to 38.2% in tensile strength of the composite [4]. These studies show the importance of interfacial adhesion and demonstrate that chemical compatibility is required for a strong interface.

The presence of a stable and strong interface between matrix and reinforcement has been a general problem for fiber and particle reinforced composites [4]. Usually matrix and filler have different chemical structures, with distinct surface energies, and characteristic individual

properties which impede their direct bonding. In order to obtain sufficient interfacial strength, coupling agents are generally necessary for glass-reinforced polymer composites [4].

N.J. Capiati and R. S. Porter [5] came up with the idea of single polymer composites, where the constituents of the composite do not have compatibility problems. In one-component polymer composites, matrix and reinforcement are made from different morphologies of the same polymer [5]. Based on this suggestion, Teishev, Marom, et al. made one-component composites using polyethylenes (PE), with gel-spun ultrahigh MW PE fibers ( $T_m = 150^\circ \text{C}$ ) and high density PE matrix ( $T_m = 130^\circ \text{C}$ ) [6-8]. However, the mechanical properties of the UHMWPE/HDPE composites were not found to be superior to two-component composites made with UHMWPE fibers and chemically dissimilar matrix polymers. In addition, single component composites might potentially be fabricated using reinforcement fibers made from stereo-complexed polymers, such as poly (L- and D-lactic acids) (PLLA and PDLA) [9], or isotactic (i) and syndiotactic (s) poly(methyl methacrylates) (PMMA) [10], which have  $T_m$ s above either of their pure stereoisomeric crystalline polymers or the  $T_g$ s of their stereoirregular amorphous polymers. However, while stereo-complexed PLLA/PDLA fibers can be melt spun [11], i- and s-PMMA cannot, but instead have recently been electrospun from solution [10]. Furthermore, these stereo-complexed fibers are not likely to be fully compatible with matrices made with their stereoirregular amorphous or stereoregular semi-crystalline counterparts.

Each of these approaches relies on the higher melting temperatures of highly oriented and crystalline gel-spun UHMW PE or stereocomplexed PLLA/PDLA or i-PMMA/s-PMMA fibers in comparison to the melting or softening temperatures of their chemically identical or closely

similar matrix polymers. As such, their composites must be formed at temperatures above the softening temperatures of the matrix and below the melting temperatures of the reinforcing fibers. As a consequence, the interfaces between them, though potentially compatible, are likely not very highly interpenetrating and strong, because the reinforcing fibers remain solid and immobile as the matrix polymer is melt-processed into them.

A second method for producing single polymer composites is the partial melting/hot compaction method [12-14]. Here there is only one starting material, generally a woven fabric. In subsequent processing, two different morphologies are obtained by partially melting the initial material. By using this technique, a variety of single-component polymer composites were produced with different polymers including PE, PP, PET, PMMA, N6,6 and N6. For example, Gong and Yang [14] took a N6 fabric, and partially melted it. They state that only the surfaces of the fibers melt, where there is higher free volume and lower crystallinity than the core of the fibers. These partially melted outer fiber surfaces act as glue and bind the remaining un-melted structure together, as schematized in Figure 1.

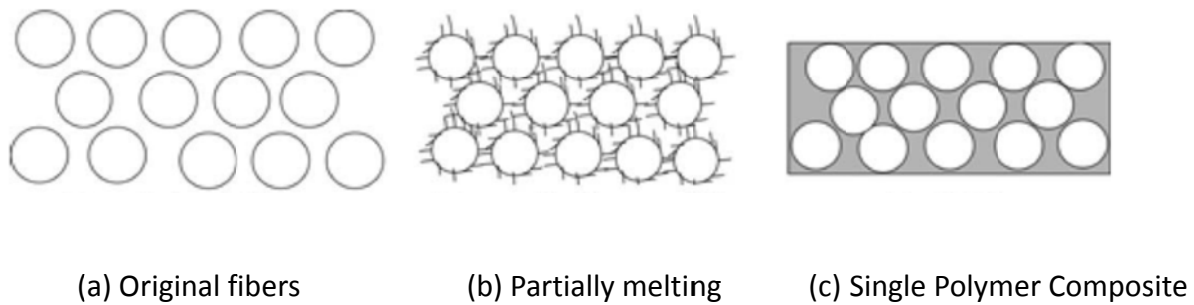


**Figure 1. Diagram of preparing single polymer composite by the partial melting method [14].**

In this technique, the matrix of the composite are the partially melted portions (dark regions in Figure 1(c)), and the remaining un-melted regions (circles in Figure 1 (c)) theoretically reinforces and supports the composite. During the partially melting process, lateral pressing or radial winding is required to prevent relaxation of high fiber orientation during heating, which makes processing difficult. Although authors claim that high orientation of the fibers is retained after processing, there is no evidence that the non-melted parts are crystalline regions, or that melted parts are totally amorphous. Nevertheless, there is still an increase in the tensile strength compared to the initial fabric. This is not unexpected, because the initial material is a fabric and final product is a film, where there are more contact points, and is denser than fabric, as seen in Figure 2.

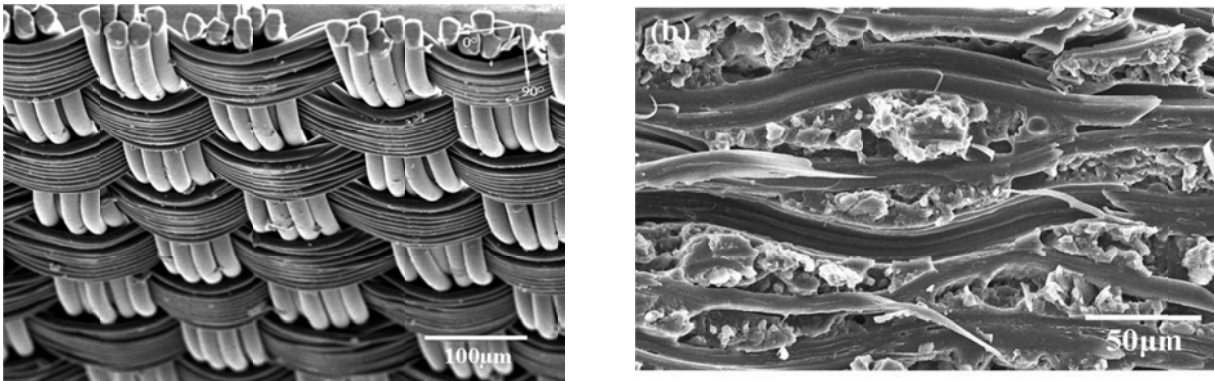


**Figure 2. Plain N-6 cloth (left hand side) and cross-section morphology of plain N-6 cloth partially melted at 226 °C (right hand side) [14].**

The process variables in the partial melting method are the temperature, pressure, and time of compaction. Precisely controlling the processing temperature is crucial in this method. In

the case of N-6, for instance, at 228<sup>o</sup> C almost all of the structure melts, while partial melting at 226<sup>o</sup> C yields the highest tensile strength [14].

In conclusion, currently two main methods exist to produce one-component polymer composites. In the first method two chemically identical polymers are required, but their melting point difference prevents the development of a strong interface. In the second method there is no matrix initially, but it forms after partial melting. In the latter case, the reinforcing unit doesn't have superior properties. Production of single-component polymer composites may be possible by combining the advantages of both techniques. A better technique requires chemically identical matrix and reinforcing components, but with both melting during processing. In addition, the reinforcing component must have mechanical properties superior to the matrix.

Employing as-received polymer as matrix and self-nucleated polymer as reinforcing unit might result in a better method to produce single-component polymer composites. As-received and self-nucleated polymers have the same melting temperature and nucleated polymers have better mechanical properties than as-received polymers. The details and the processing procedures for this type of composite are the subjects of the following chapter.

## REFERENCES

1. Lee SM. Dictionary of composite materials technology. 1989.
2. Hull D, Clyne TW. An Introduction to Composite Materials, 2nd Edition, Cambridge Solid State Series. 2003.
3. Currey, J. D. Biological composites, in Handbook of Composites, vol. 4 – Fabrication of Composites. Kelly A, Mileiko ST (eds.). Elsevier: New York, pp.501-64. 1983.
4. Mobarakeh HS, Kadi AA, Brisson J. Improvement of mechanical properties of composites through polyamide grafting onto Kevlar fibers, *Polymer Eng. & Sci.* Vol. 36, No. 6. 1996.
5. Capiati NJ, Porter RS. Concept of one polymer composites modeled with high-density polyethylene, *J. Mat. Sci.*, 10, 1671-77. 1975.
6. Teishev A, Incardona S, Migliaresi C, Marom G. Polyethylene fibers/polyethylene matrix composites-Preparation and physical properties, *J. Appl. Polym. Sci.*, 50, 503-12. 1993.
7. Teishev A, Marom G. The effect of transcrystallinity on the transverse mechanical properties of single-polymer polyethylene composites, *J. Appl. Polym. Sci.*, 56, 959-66. 1995.
8. Stern T, Marom G, Wachtel E. Origin, morphology, and crystallography of transcrystallinity in polyethylene-based single-polymer composites, *Composites, Part- A, Appl. Sci. Manufactor*, 28, 437-44. 1997.

9. Hyon H, Jamshidi K, Ikada Y. In *Polymers as Biomaterials*; S. W. Shalaby, A. S. Hoffman, B. D. Ratner, T. A. Horbett, Eds.; Plenum Press: New York, London, 1984; pp 51.
10. Crne M, Park JO, Srinivasarao M. Electrospinning Physical Fels: The Case of Stereo complex PMMA, *Macromolecules*, 42, 4353-55. 2009.
11. Furuhashi Y, Kimura Y, Yamane H. Higher order Structural Analysis of Stereocomplex Poly(lactic acid) Melt-Spun Fibers, *J. Polym. Sci. Part B-Polym. Phys*, 45, 218-28. 2007.
12. Hine PJ, Ward IM, Olley RH, Bassett DC. The Hot Compaction of High Modulus Melt-Spun Polyethylene Fibres, *Journal of Materials Science*, vol.28, pp.316-324. 1993.
13. Ward IM, Hine PJ. Novel composites by hot compaction of fibers, *Polymer Engineering & Science*, 37: 1809–1814. doi: 10.1002/pen.11830. 1997.
14. Gong Y, Yang G. Single polymer composites by partially melting recycled polyamide 6 fibers: Preparation and characterization. *Journal of Applied Polymer Science*, 118: 3357–3363. doi: 10.1002/app.3236. 2010.

## CHAPTER 3

# Producing Single-Component Polymer Composite by Using Coalesced Polymer

### 3.1 Introducing a new method to produce single-component polymer composites

The importance of the interfacial strength between matrix and reinforcing unit was discussed in the previous chapter. Single polymer composites potentially have better interface performance than traditional glass or carbon fiber reinforced polymer composites [1]. Single-component polymer composites not only eliminate the interface problem, but also simplify recycling of composite materials [1].

The two current methods for producing one-component polymer composites have been discussed. In the first method, there are two chemically identical polymers with different melting points. In this technique one constituent melts while the other constituent doesn't. This is a disadvantage because strong interfaces cannot be obtained if both components do not melt at the same time. In the second method, partial melting of the structure provides stronger interfaces, because both components melt at the same time. This technique, however, does not initially have separately matrix and reinforcing units. Un-melted parts of the initial material create the reinforcing units after the partial melting process. Although studies show some increase in tensile properties, this is not likely because of a strong reinforcing unit, but because of the stronger

interface compared to the initial material. Our aim is producing a single-component self reinforced polymer composite with both strong reinforcing units and strong interfaces.

This type of self-reinforced composite would be produced by making the reinforcing component from the same polymer as the matrix, but with the constituent polymer chains in the reinforcing unit organized in a way that prevents their substantial diffusion into the matrix polymers during their melt-processing into a single-component composite. Such a reorganization of polymer chains may be achievable by nucleating the melt crystallization of polymers with guest polymers coalesced from their crystalline inclusion compounds (ICs) formed with the host cyclic starches, cyclodextrins (CDs).

As we discussed in Chapter I, coalesced polymers have properties distinct from as-received polymers. They have higher crystallinity and higher crystallization temperatures due to their extended conformations and untangled nature. Moreover, they retain their coalesced structures and morphologies even after spending long times in their melts [2].

We seek to learn whether or not single-component polymer composites can be fabricated with a nucleated reinforcing unit made with the addition of a small amount (a few wt %) of coalesced polymer and the same un-nucleated polymer as the matrix. Two critical questions require answers. First, does the composite that we make by using nucleated polymer and bulk polymer becomes a single phase material after melt processing? If they mix completely after melt processing, this material won't be a composite, because composites have to be multiphase materials, by definition. Second, do these nucleated reinforcement polymers provide better mechanical properties? This is important because if we cannot obtain improved mechanical

properties, this method would be the same as the partial melting hot compaction method, where we have strong interfaces but only modest reinforcement.

In order to answer these two critical questions we have chosen to use Nylon-6 (N-6) in our self reinforced composites, where as-received N-6 is the matrix and nucleated (nuc) N-6 is the reinforcing unit. A flow diagram that summarizes our study is presented in Figure 1.

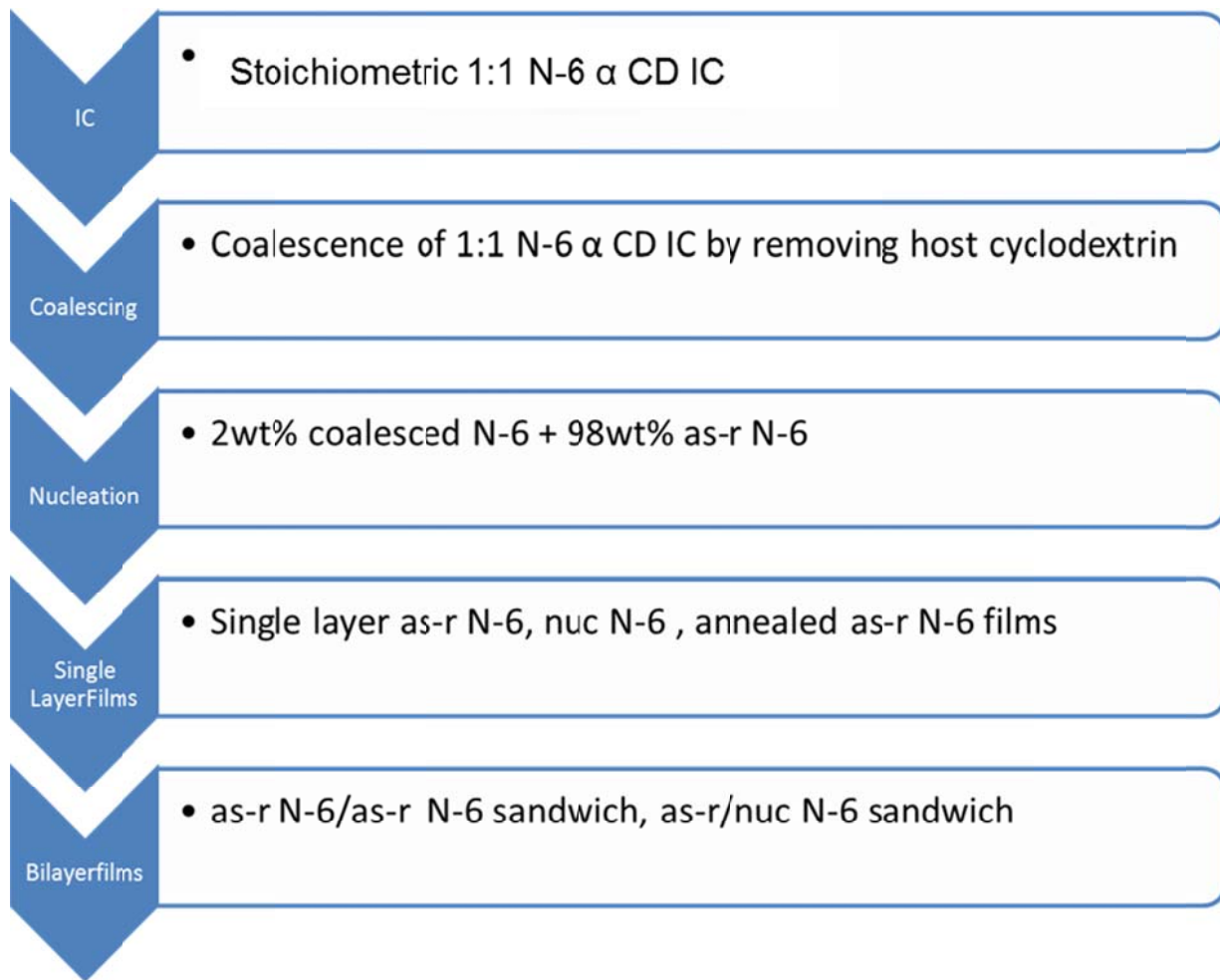


**Figure 1. Flow diagram of this study.**

First we successfully inserted all guest N-6 chains into host nano-sized ( $\sim 0.5\text{nm}$ )  $\alpha$ -cyclodextrin ( $\alpha$  CD) channels, resulting in stoichiometric 1:1 N-6  $\alpha$  CD ICs. Coalesced N-6 was obtained by removing the host cyclodextrin channels, and were used as nucleating agents by adding a few wt % to as-received (as-r) N-6. In order to compare mechanical properties of as-r N-6 and nuc N-6, thin films were made and tensile tests were conducted. Once we determined that nuc N-6 has better mechanical properties than as-r N-6, we decided to use it as reinforcing unit for our self reinforced composite. Single-component polymer composites were made into a sandwich of the two films, with one layer of as-r N-6 and one layer of nuc N-6. Note that as-r N-6 and nuc N-6 are chemically identical but possess different morphologies.

## **3.2. Experimental**

### **3.2.1. Materials**

N-6 having a molecular weight of 60,000 was obtained from BASF (brand name Ultramid B4001<sup>®</sup>). All solvents were obtained from Sigma-Aldrich,  $\alpha$ -cyclodextrin was obtained from Cerestar Co, and Film Made of Teflon<sup>®</sup>PTFE was obtained from McMaster-Carr.

### **3.2.2. Methods**

#### **3.2.2.1. Inclusion Complex Formation**

Stoichiometric (s) 1:1 N-6- $\alpha$ -CD-IC were produced with a slightly different technique than our previous work [3,4,5]. In previous studies, 0.5 g of N-6 were used, but here 2 g of N-6 was dissolved in 60 mL of 90% formic acid at room temperature. Different than the previous studies, we didn't add acetic acid after dissolving N-6. A total of 17.08 g of  $\alpha$ -CD was dissolved

in 84 mL of 99% dimethyl-sulfoxide. Once  $\alpha$ -CD dissolved completely, the  $\alpha$ -CD solution was added to the N-6 solution. Their combined solution was stirred and heated on a hot plate at 50 °C for 2 h, then cooled to room temperature, and continuously stirred for another 6 h. The precipitate was vacuum filtered and rinsed with formic acid and deionized water and finally dried in a vacuum oven for 24 hours.

### **3.2.2.2. Coalescence Process**

The coalescence process to remove the host cyclodextrin channels of 1:1 N-6- $\alpha$ -CD-IC was accomplished by stirring the IC in excess deionized water for 2 h. In this process coalescence occurs faster if the particle size of precipitated IC is small. After coalescence the N-6 obtained has a different morphology than as-received N-6.

### **3.2.2.3. Nucleation Process**

Nucleated Nylon-6 was obtained by a solvent casting method. After N-6 was dissolved in 90% formic acid, coalesced N-6 was added into the solution. Finally formic acid was removed by evaporation, and the remaining nucleated Nylon-6 was processed into a powder in a blender and dried in a vacuum oven for 24 hours.

### **3.2.2.4. Film Production**

Four different classes of films were produced by placing appropriate material on a constraining, non-stick Teflon<sup>®</sup> sheet. First we produced two kinds of single layer films. 1g of N-6 pellets and 1 g nucleated N-6 powder were melt pressed under applied pressure of 1.75 MPa for 6 minutes, to produce single layer as-r N-6, and single layer nuc N-6 films, respectively.

Using these single layer films two types of bilayer sandwich films were produced. First we produced two layers of as-r N-6 by melt pressing 1 g of as-received film onto 1 g of as-received film (2 Layers of as-r N-6). Our second type of bilayer film was produced by melt pressing 1 g of as-received single layer film onto 1 g of nucleated N-6 film (single-component polymer composite). Bilayer films were melt-pressed under an applied pressure of 2.62 MPa for 1 minute at 240 °C.

### **3.2.3. Experimental Techniques**

#### **3.2.3.1. Fourier Transform Infrared Spectroscopy**

Infrared spectral studies were conducted with a Nicolet 510P FTIR spectrometer. Observations were conducted in the range 4000-400  $\text{cm}^{-1}$ , with a resolution of 4  $\text{cm}^{-1}$ . Powdered  $\alpha$ -CD, N-6, stoichiometric N-6- $\alpha$ -CD-IC, and coalesced N-6 samples were pressed into KBr pellets for the FTIR absorption measurements [4]. 64 scans were conducted for all measurements. FTIR data were analyzed by using Omnic software.

#### **3.2.3.2. Differential Scanning Calorimeter**

Differential scanning calorimetric (DSC) thermal scans were performed with a Perkin Elmer Diamond DSC-7 instrument. Hermetically sealed aluminum pans were used in all experiments. The measurements were run in the range 25-250 °C at a heating and cooling rate of 10 °C/min. All samples were held at 250 °C for 5 minutes before the cooling scan. Nitrogen was used as the purge gas [4].

DSC data were analyzed by using Pyris software. For a combination of heating and cooling curves, approximately 50,000 data points were collected. Melting and crystallization temperatures and enthalpies were calculated automatically by the software from the areas of endothermic and exothermic peaks. The degree of crystallinity was calculated with the formula shown below (Eq. 1):

$$\text{Degree of crystallinity (\%)} = \frac{\Delta H_f}{\Delta H_f^\circ} \times 100 \quad (1)$$

Where  $\Delta H_f$  is the heat of fusion observed for the sample, and  $\Delta H_f^\circ$  is the heat of fusion of 100% crystalline Nylon-6 which is taken as 160 J/g [4].

### **3.2.3.3. Wide Angle X-Ray Diffraction**

Wide Angle X-Ray Diffraction studies were performed with a Siemens type -F X-ray diffractometer equipped with a Ni-filtered  $\text{CuK}_\alpha$  radiation source ( $\lambda=1.54\text{\AA}$ ). The supplied current and voltage were 30kV and 20mA, respectively, and diffraction intensities were measured every  $0.1^\circ$  from  $2\theta=5$  to  $30^\circ$  at a rate of  $(2\theta=3^\circ)/\text{minute}$  [4].

### **3.2.3.4. Tensile Tests**

Tensile tests were conducted according to ASTM D-882-97 using a MTS Q-Test<sup>TM</sup>/5, CRE-type tester. The test specimens were prepared by cutting .14-.15mm thick films into 6mm wide and 90mm long dog bone shapes using a template (see Figure 2). Tensile tests were performed using a 250lb load cell, and the gauge length was 50mm. The cross-head speed must be adjusted according to the elongation at break. Our initial experiments showed that single layer

as-r N-6 and two layer as-r N-6 films had percent strain at break values greater than 100. This is why cross-head speed was 500mm/min for these films. In the case of single layer nuc N-6, annealed N-6 and two layer as-r/nuc N-6 films, cross-head speed was 50mm/min, because these films showed a much lower percent elongation at break. Modulus values were calculated from the initial part of the load-elongation curve where the slope is constant. The load- strain curve, modulus, peak load, break load, yield load, strain at peak load, strain at break load, elongation at break, and energy to break data were acquired at the end of each test, and each value of the mechanical properties reported was an average of at least five film test specimens. Breaks that occurred very close to the gauche clamps or were initiated by flaws were not included in the test results. Sample shape and dimensions are depicted in Figure 2.

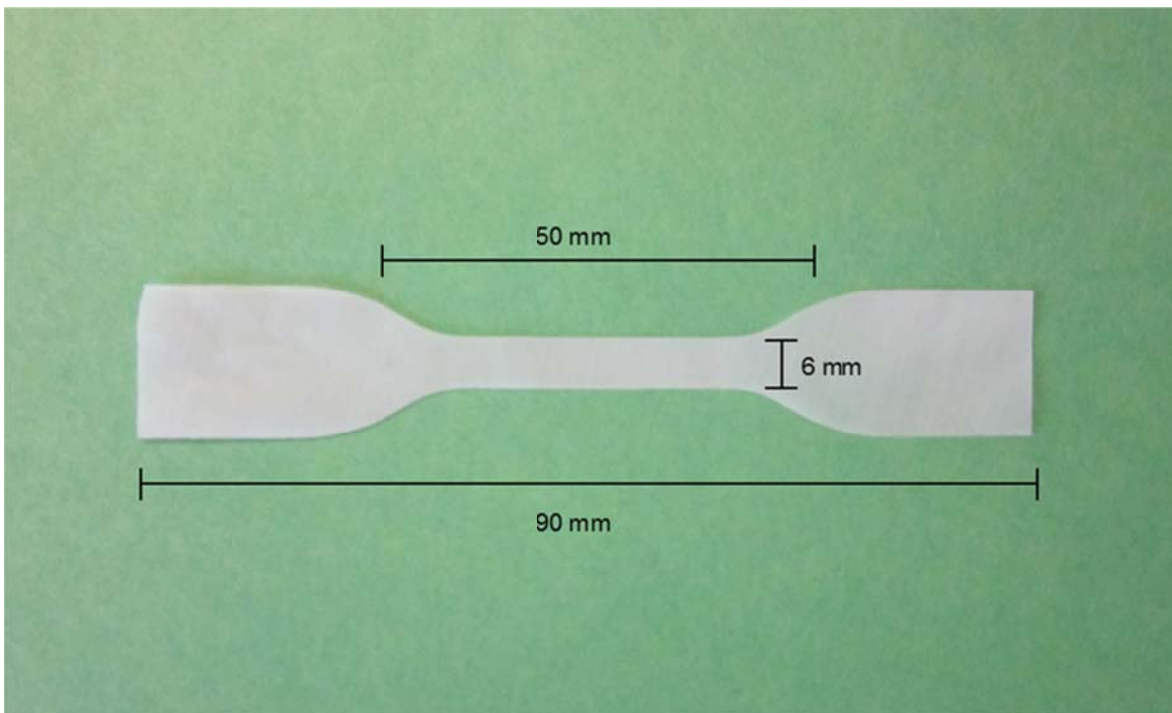


**Figure 2. Picture of a dog bone specimen for tensile test.**

### 3.2.3.5. Density Measurements

Densities of as-r N-6 and coalesced N-6 were determined by floatation in a mixed solution of carbon tetrachloride (CT) and toluene (T), whose densities are greater ( $\rho_{CT} = 1.594 \text{ g/cm}^3$ ) and less ( $\rho_T = 0.8668 \text{ g/cm}^3$ ) than N-6. Small portions of N-6 film were floated atop 25ml of CT in a 100ml graduated cylinder containing a magnetic stir bar that was placed on a magnetic stir plate. The tip of a 50ml burette containing T was inserted through aluminum foil that covered the mouth of the graduated cylinder. While stirring, T was slowly dripped in (~10 drops/ml) until the N-6 film sank below the surface of and became suspended in the CT/T solution when stirring was stopped. The volume of T,  $\text{vol}(T)$ , required to achieve suspension of the N-6 sample was then used to determine the N-6 film density,  $\rho_{N-6}$ , from equation 2.

$$\rho_{N-6} = [\text{vol}(T)\rho_T + 25\rho_{CT}]/[\text{vol}(T) + 25] \quad (2)$$

Comparative N-6 film densities were observed for melt-crystallized as-received and coalesced N-6 samples possessing the same crystallinity, as determined by DSC. This was achieved by simultaneously placing a portion of each of the N-6 melt-crystallized films in the graduated cylinder containing CT, and adding T as just described. The film that first began to sink and became suspended in the CT/T column had the highest density, which must be attributed to closer packing of chains in the non-crystalline regions of the sample [5].

### 3.2.3.6. Scanning Electron Microscope

Scanning electron microscope (SEM) images were recorded on the N-6 film sandwiches using a FEI Phenominstrument. The film sandwiches were placed onto specimen mounts with

double sided conductive carbon tape and coated with gold/palladium to reduce charging. A Quorum Technologies SC7620 Mini Sputter Coater was employed for 45 seconds.

### **3.2.3.7. Polarized Optical Microscope**

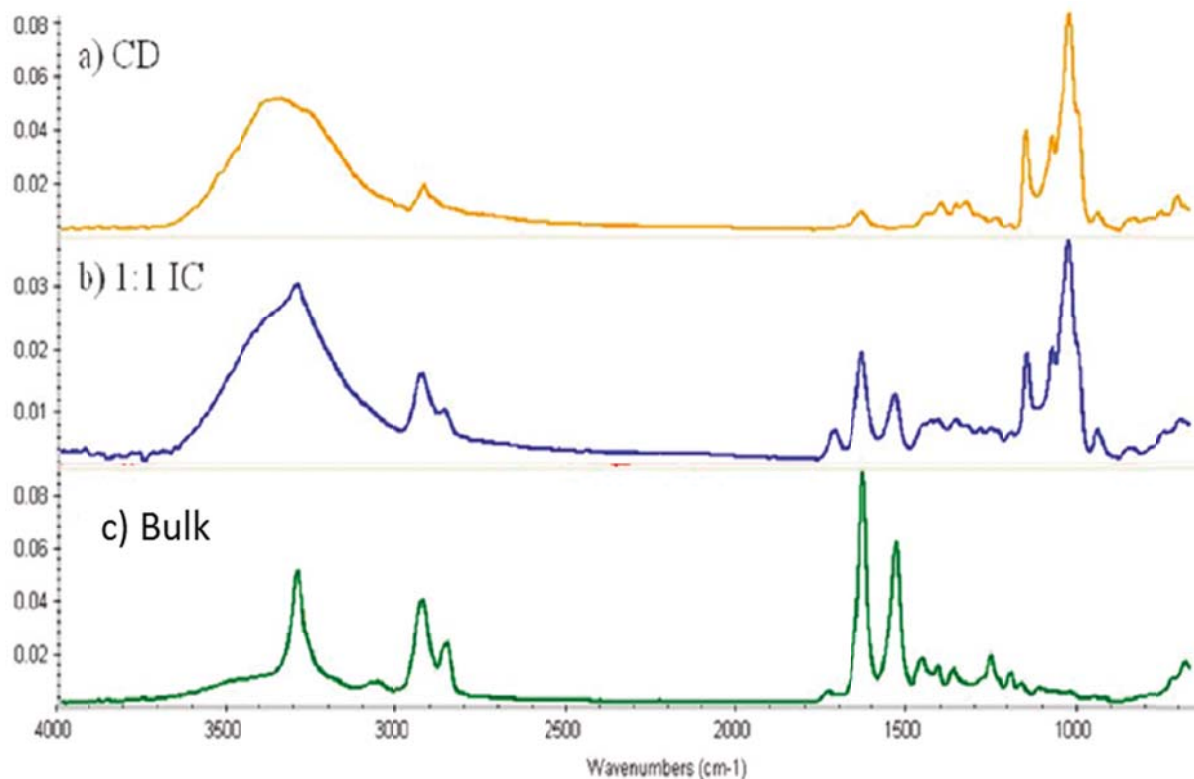
Polarized optical microscopic observation for various films were performed on a Nikon Eclipse 50i POL Optical Microscope equipped with a CCID-IRIS/RGB color video camera made by Sony Corp.

## **3.3. Results and Discussion**

### **3.3.1. Characterization of the Nylon 6 $\alpha$ -Cyclodextrin Inclusion Complex**

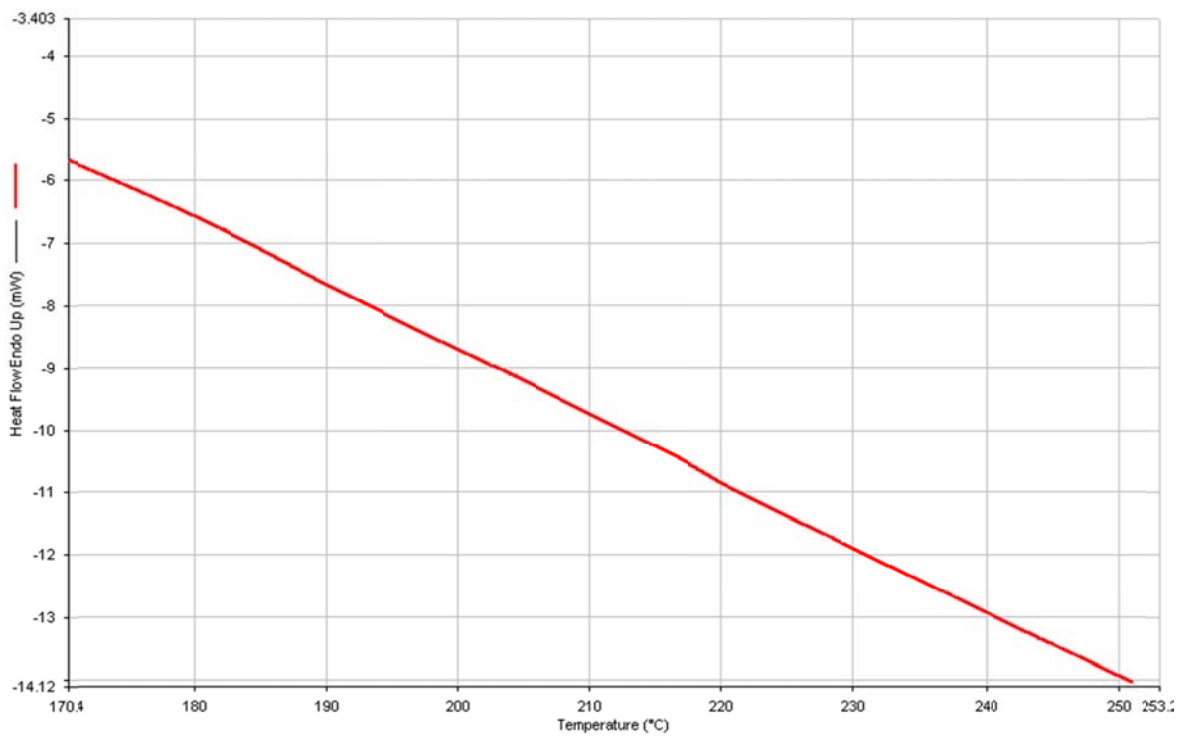
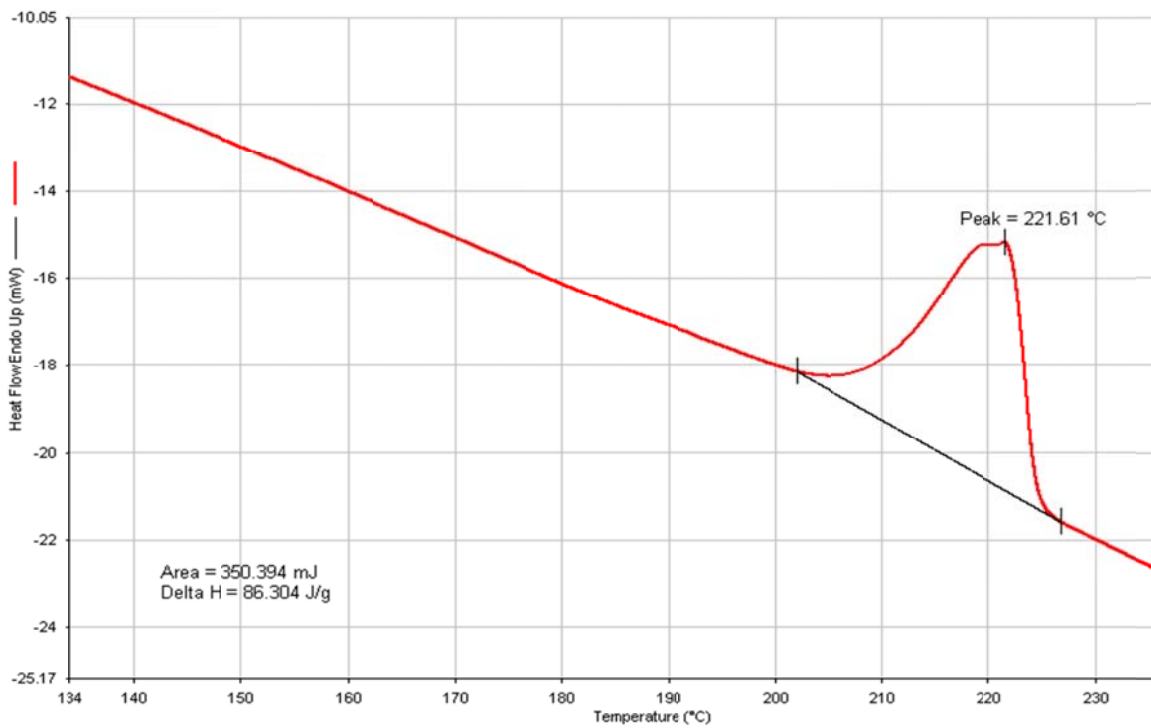
We employed three analytical techniques to confirm that we had produced a stoichiometric 1:1 N-6- $\alpha$ -CD inclusion complex. These techniques are FTIR, DSC, and X-ray.

Figure 3 shows the characteristic FTIR absorption peaks for  $\alpha$ -CD (a) and as-r N-6 (c). Since Figure 3 (b) has the specific peaks from both  $\alpha$ -CD and as-r N-6, we can say that we have both components in our N-6- $\alpha$ -CD-IC sample, but we cannot say whether we have an IC or physical mixture of  $\alpha$ -CD and N-6.



**Figure 3. FTIR scans for  $\alpha$ -CD (a), 1:1 N-6  $\alpha$ -CD-IC (b), and bulk N-6 (c).**

After confirming that we have both  $\alpha$ -CD and N-6 in our precipitate, we conducted DSC. If DSC does not show an as-r N-6 melting peak, as can be seen in Figure 4, we can state that our precipitate is an IC and not a physical mixture. The stoichiometric IC does not show as-r N-6 melting, because melting requires crystalline N-6. Since there are only single extended N-6 chains arranged inside the  $\alpha$ -CD channels, we do not have any possibility for crystallinity. Moreover, the N-6 chains inside the cyclodextrin channels are isolated by the  $\alpha$ -CD channels up to 300 °C, after which the  $\alpha$ -CD channels melt and decompose [10].



**Figure 4. DSC heating scans for as-r N-6 (upper), 1:1 N-6  $\alpha$ -CD-IC (lower).**

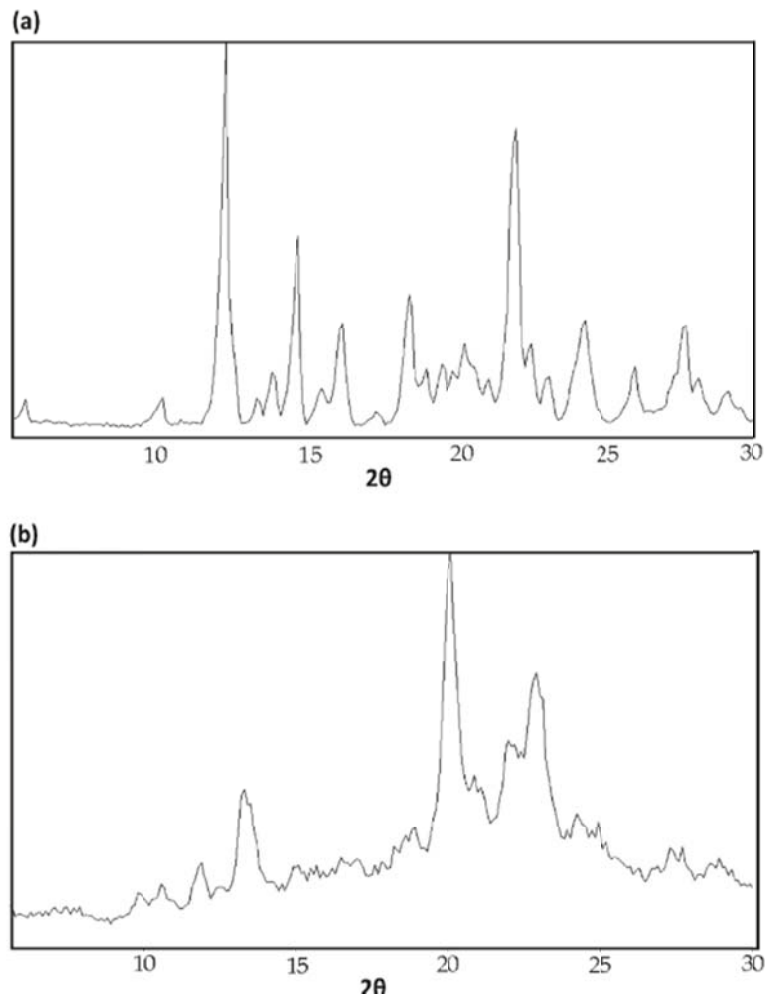


**Figure 5. WAXD of cage crystalline structure of pure  $\alpha$ -CD (a) and columnar crystalline structure of N-6- $\alpha$ -CD-IC.**

Although FTIR and DSC are sufficient to confirm IC formation, X-ray observations were also conducted. As seen in Figure 5, the N-6- $\alpha$ -CD-IC has a columnar structure, which is likely possible only when guest polymer chains are included inside the host  $\alpha$ -CD channels. If there were no inclusion, then  $\alpha$ -CD would adopt a cage crystalline structure with the corresponding characteristic XRD pattern, as discussed in Chapter I.

### 3.3.2. Coalescence and Characterization of Nylon 6

Confirmation of N-6 coalescence was done by FTIR and its properties were investigated by DSC, X-ray, and density tests.

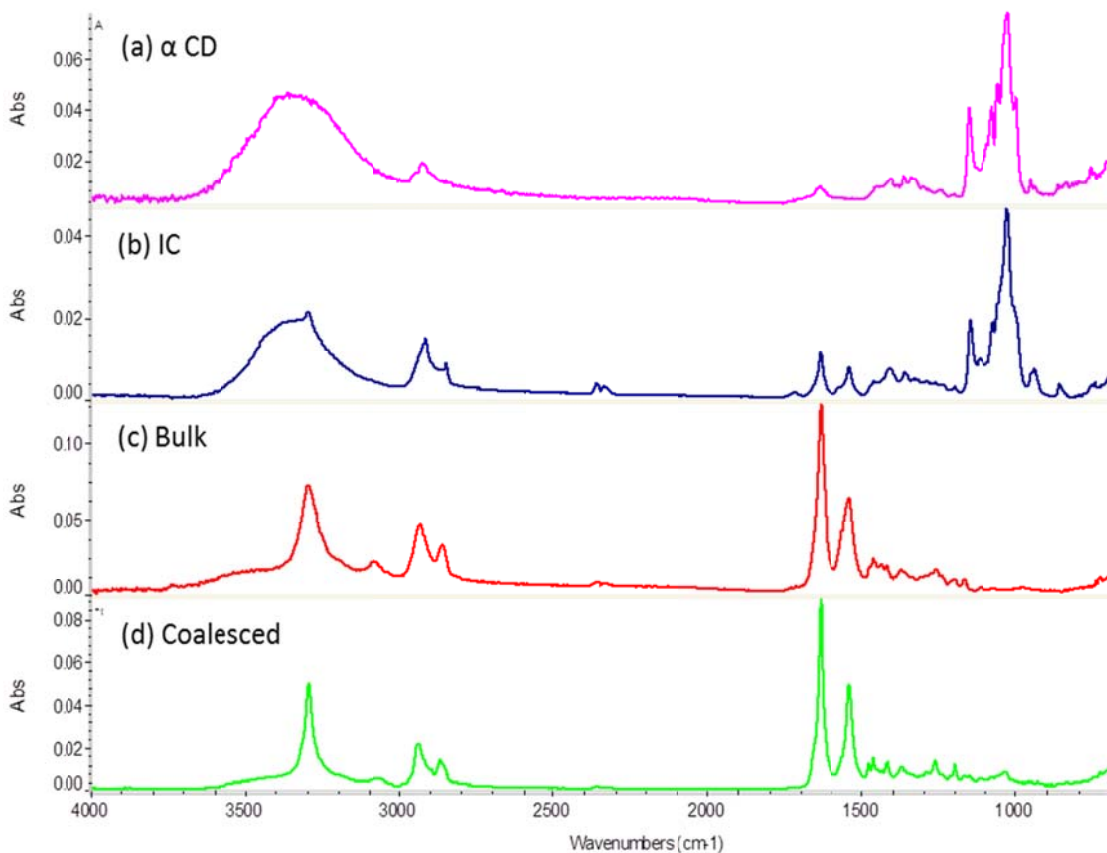


**Figure 6. FTIR scans of  $\alpha$ -CD(a), 1:1 N-6 of  $\alpha$ -CD IC (b), as-r N-6 (c), and coalesced N-6 (d).**

Coalesced and as-received polymers are chemically identical. Therefore, the FTIR scan of coalesced N-6 should be the same as as-r N-6. More importantly, there should not be any trace of remnant  $\alpha$ -CD present. As seen in the FTIR spectra in Figure 6, there is no  $\alpha$ -CD in the

coalesced N-6, because it only shows the same absorption peaks as as-r N-6. In addition, note the superior resolution of the spectrum for coalesced N-6. This results from both its greater crystallinity and the un-entangled and extended nature of N-6 chains in the non-crystalline sample regions [9].

As we discussed in previous chapters, the coalescence process leads to distinct properties. Figure 7 shows DSC heating and cooling scans of coalesced N-6, while as-r N-6 has a  $T_c$  at 167 °C, coalesced N-6 crystallized at 186.5 °C (compare with Figure 10 in next section). In addition, crystallization takes place over a narrower temperature range leading to a more uniform semi-crystalline structure.

Moreover, coalesced N-6 has a crystalline structure distinct from as-r N-6. Depending on the cooling rate, N-6 can adopt either the  $\alpha$ - or  $\gamma$ -polymorphs. The  $\alpha$ -polymorph occurs upon slow cooling the N-6 melt, while quenching results in the  $\gamma$ -polymorph. The main difference between these two crystal structures is the orientation of N-6 chains in the unit cell. In the  $\gamma$ -polymorph hydrogen-bonded N-6 chains are oriented parallel to each other, while they are anti-parallel in the  $\alpha$ -polymorph [6]. As depicted in Figure 8, the anti-parallel chains in the  $\alpha$ -polymorph enable more linear and stronger H-bonds. Since the strength of a hydrogen bond is only one tenth of a covalent bond, one can easily underestimate their importance. However, they increase the strength of polyamides significantly due to their vast numbers.

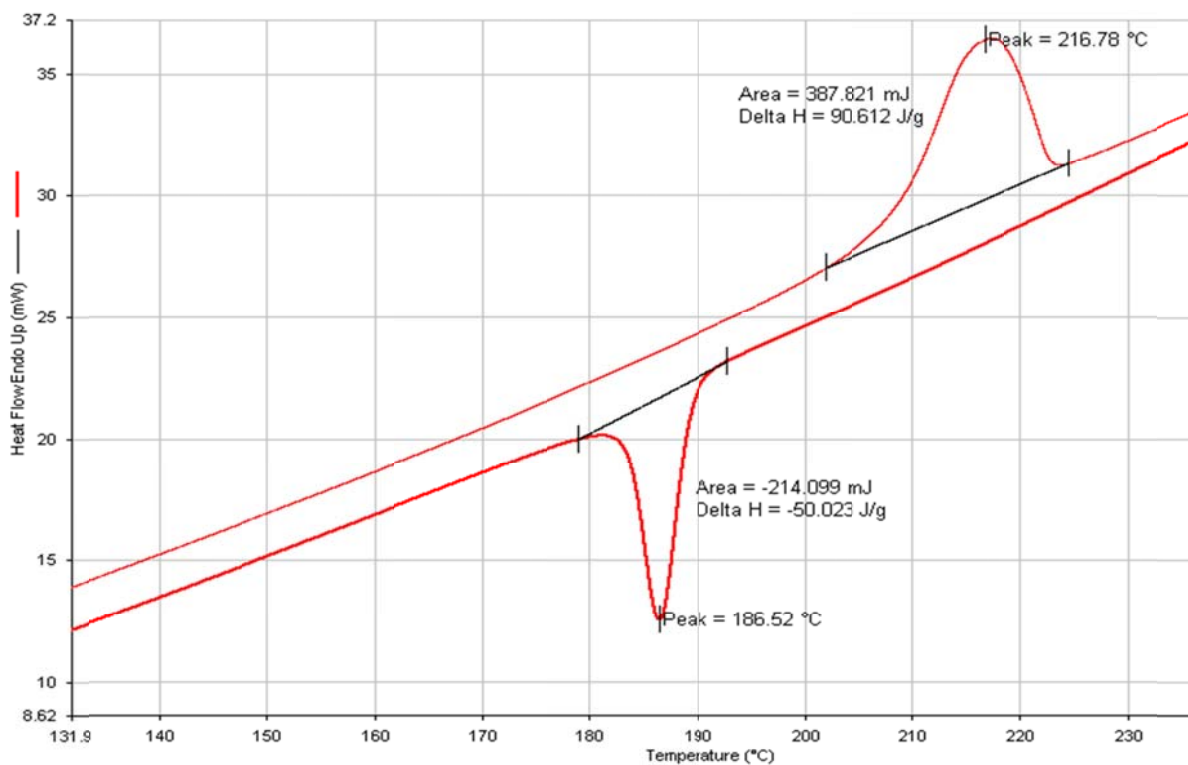


Figure 7. DSC heating and cooling scans for coalesced N-6.

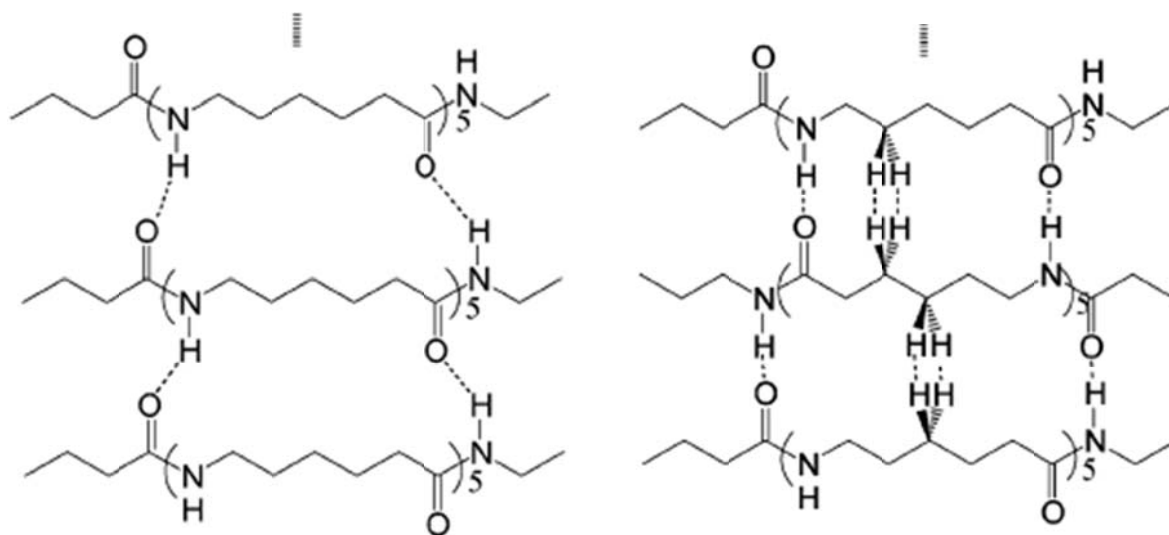
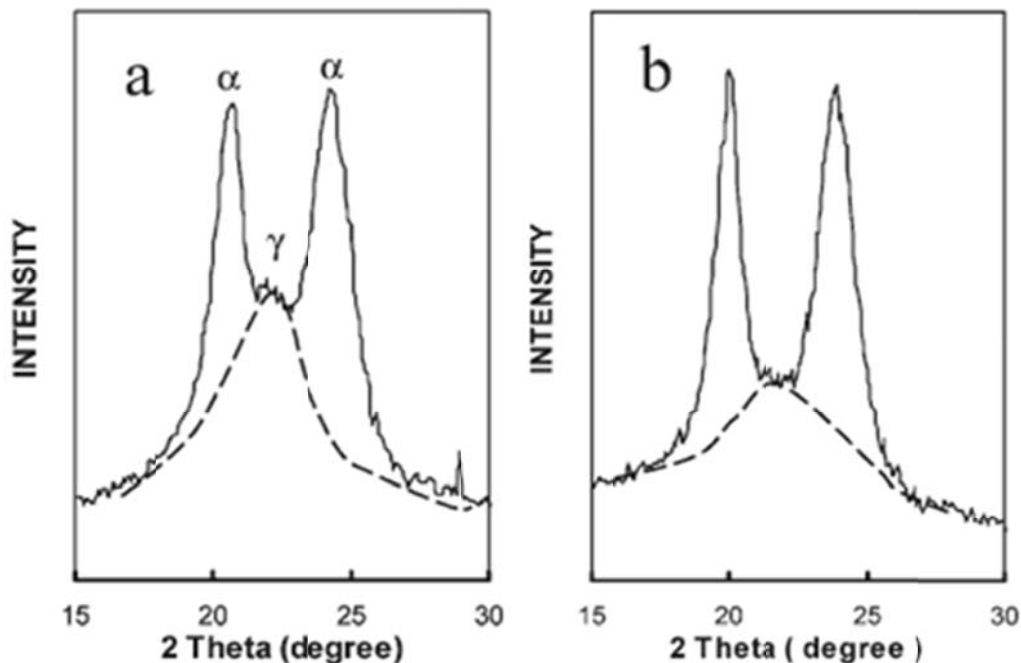


Figure 8. Parallel ( $\gamma$ , left) and anti-parallel ( $\alpha$ , right) N-6 chains [7].

The X-ray diffraction patterns of  $\alpha$ - and  $\gamma$ -polymorphs have their own two characteristic peaks at room temperature. While the  $\alpha$ -polymorph shows peaks at about  $2\theta=20$  and  $23.7^\circ$ , the  $\gamma$ -polymorph show two peaks at about  $2\theta=10.7^\circ$  (Not shown) and  $21.4^\circ$ . As seen in Figure 9, the amount of  $\gamma$ -phase significantly decreases upon coalescence [4].



**Figure 9: WAXD scans for as-r (left) and coalesced (right) N-6 [4].**

Not only the crystalline regions, but also the non-crystalline regions of coalesced N-6 differ from the as-r N-6, because density measurements indicate that coalesced N-6 is denser than as-r N-6. Since their crystalline density and chemical structure are the same, only non-crystalline regions can contribute to this density increase which reflects a closer packing of N-6 chains in the non-crystalline regions. Coalescence yields extended and oriented chains and produces closer packing in non-crystalline regions. Density values are given below in Table 1.

**Table 1. Nylon-6 Densities [5].**

Material	X <sub>c</sub> (DSC crystallinity)	Density (g/cm <sup>3</sup> )
Nylon-6	0.53	1.1559
Nylon-6 ( coalesced from  1:1 N-6- $\alpha$ -CD-IC)	0.51	1.1674
Density of non-crystalline regions in Nylon-6		1.084 g/cm <sup>3</sup>
Density of non-crystalline regions in Coalesced Nylon-6		1.111 g/cm <sup>3</sup>

### 3.3.3. Employment of Coalesced Nylon 6 as a nucleating agent and Its Characterization

As mentioned previously, nucleated N-6, not pure coalesced N-6, will be our reinforcing unit. The reason is that only approximately 10% of N-6- $\alpha$ -CD-IC is N-6. It is extremely tedious to produce large amounts of coalesced polymers. However, coalesced polymers can serve as nucleating agents when a few wt % are used [4]. Here we nucleated 2g of as-r N-6 with 0.04g of coalesced N-6. The nucleated N-6 has a larger amount of crystallinity and a higher crystallization temperature (T<sub>c</sub>). As seen in Figure 10, as-r N-6 crystallized at 167 °C and nucleated N-6 crystallized at 184 °C. Similar to coalesced N-6, nuc N-6 also crystallizes over a narrower temperature range (Compare to Figure 7), yielding a more uniform semi-crystalline morphology.

Polarized Optical Microscope images, in Figure 11, indicate that nucleated N-6 crystallizes in more homogeneously providing finer scale morphology than as-r N-6.

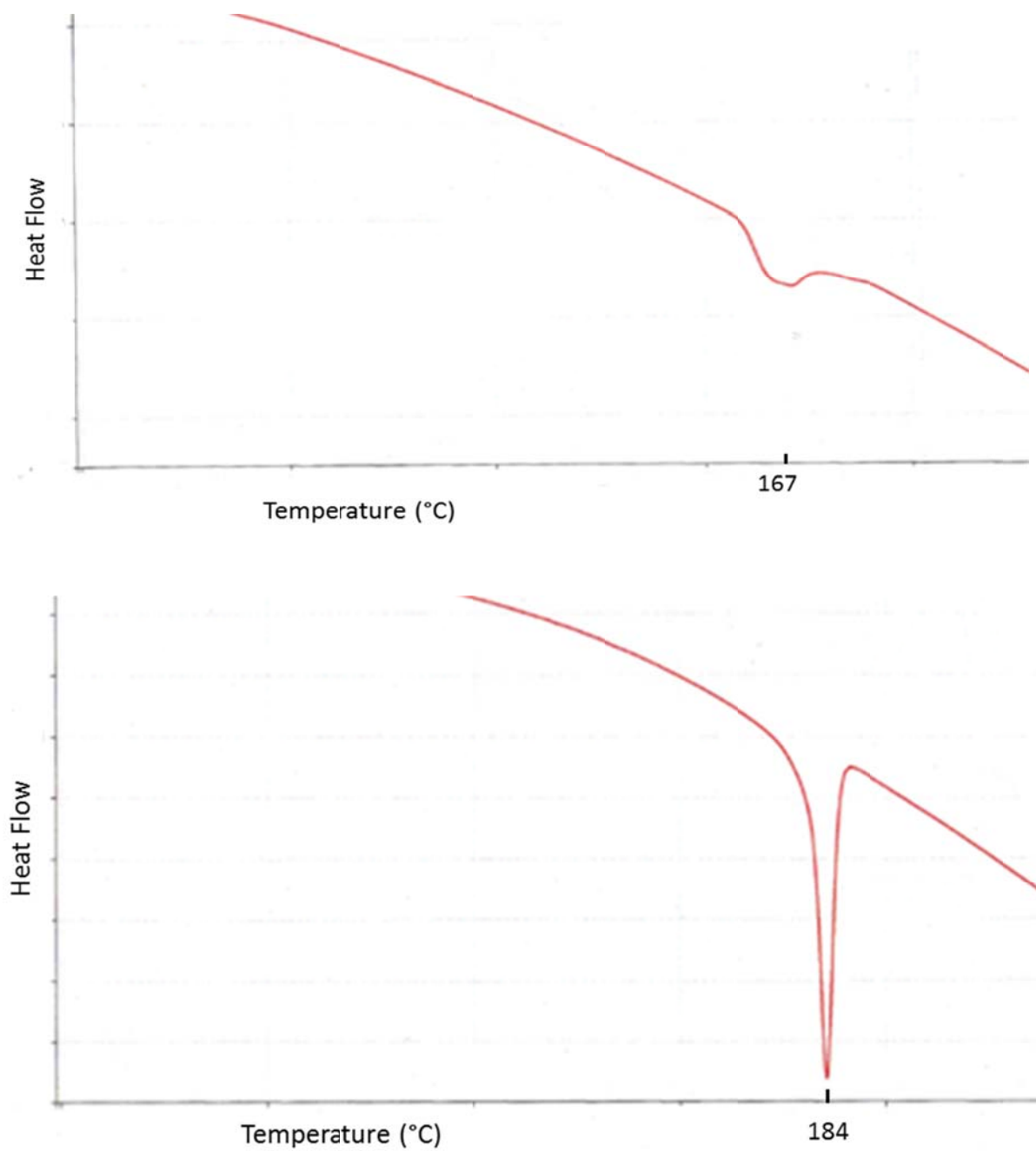


**Figure 10. DSC scans of N-6 (upper) and nuc N-6 (lower).**

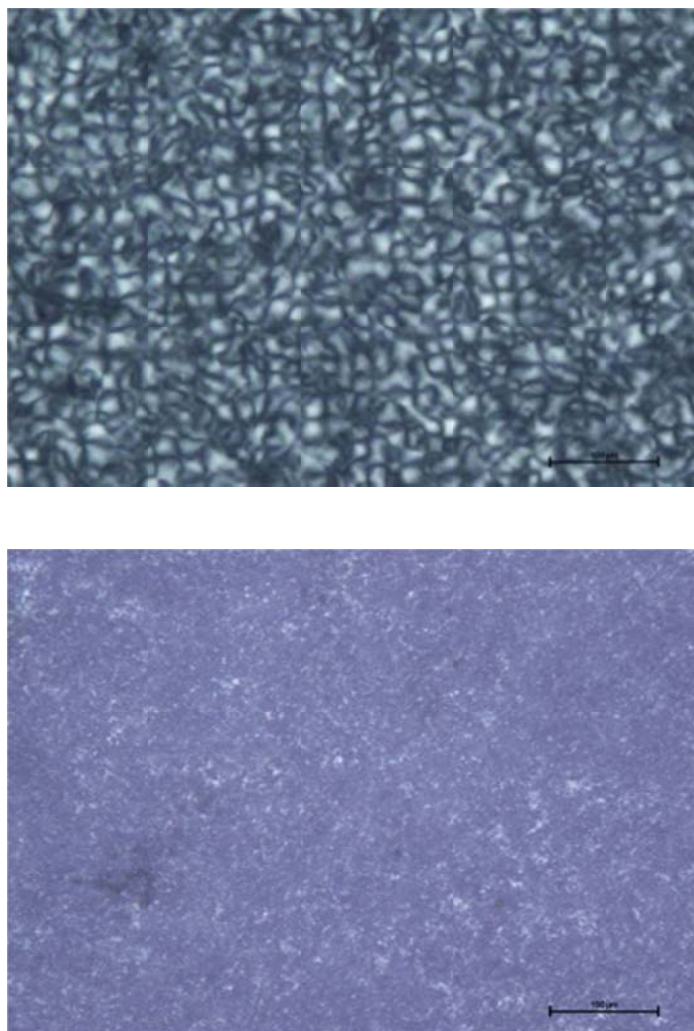


**Figure 11. Polarized Optical Microscope images for melt crystallized films of (upper) neat N-6, and (lower) nucleated N-6 with 2 wt% N-6 coalesced from 1:1 N-6-  $\alpha$ -CD-IC [6].**

#### **3.3.4. Single Layer as-r N-6 and nuc N-6 films and their characterization**

After melt pressing N-6 pellets and nuc N-6 powder between Teflon® sheets, single layered films were obtained after 6 minutes under an applied pressure of 1.75 MPa at 240 °C. DSC results of these films are shown in Figure 12. As we discussed previously, nuc N-6 has a

larger amount of crystallinity and higher  $T_c$  than as-r N-6. As anticipated, the nucleated single layer film also has a larger amount of crystallinity and higher  $T_c$  than as-r N-6. The as-r N-6 film has 36 % crystallinity, while the nuc N-6 film has 52 %.  $T_c$  of as-r N-6 pellets are 167 °C, but  $T_c$  of as-r N-6 film is 183.5 °C. Similarly  $T_c$  of nucleated films also increases to 191.5 °C from 184 °C after melt-pressing.

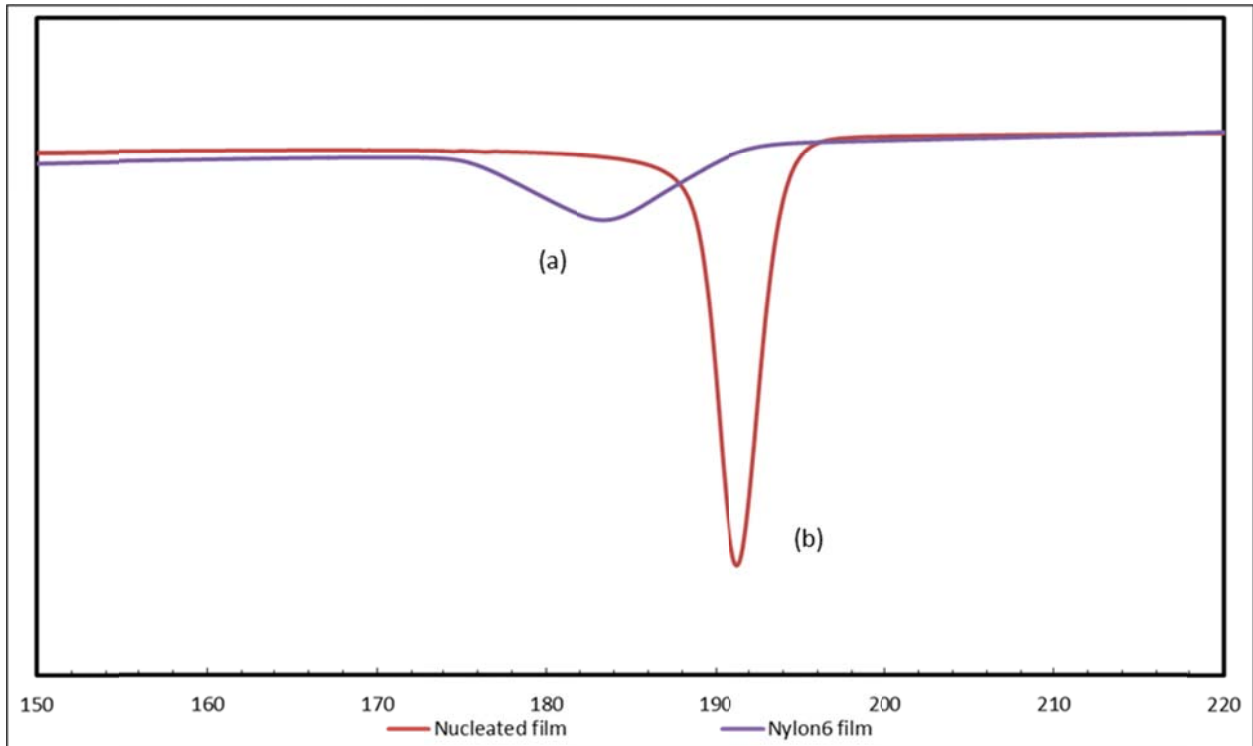


**Figure 12. DSC of single layer as-r N-6 film (a) and single layer nuc N-6 film (b).**

As we mentioned earlier, the purpose of making nucleated films is for comparing their mechanical properties with as-r N-6 films. If single layer nuc N-6 films have superior mechanical properties, then they will be used as the reinforcement layer in our one-component composites. Mechanical properties of as-r N-6 films and nuc N-6 films were examined by the Q-

Test. Tensile tests were conducted for each film as discussed in section 3.2.3.4. Typical load-strain curves for single layer as-r N-6 and single layer nuc N-6 film are presented in Figure 13.

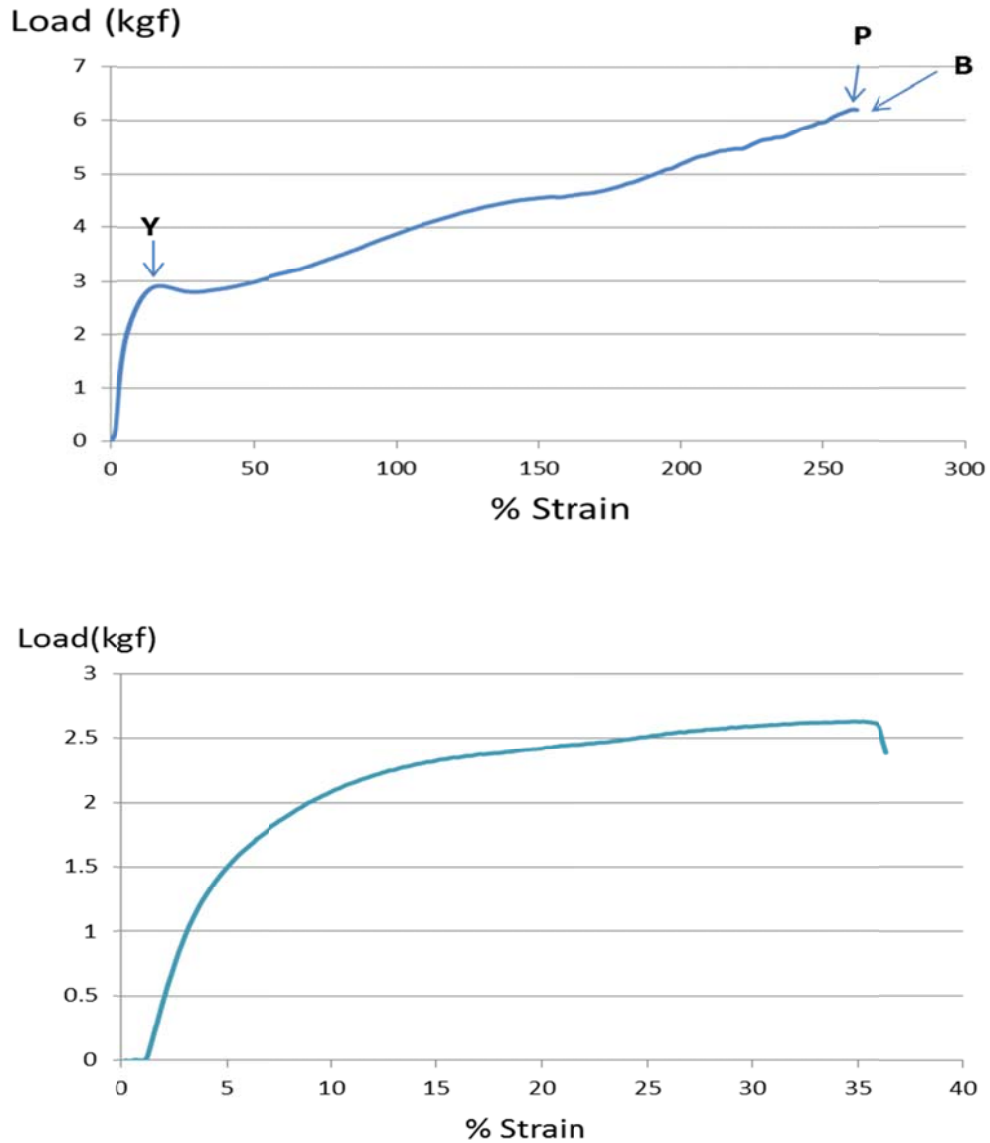


**Figure 13. Response of single layer as-r (upper) and nuc (lower) N-6 films to applied load. Yield load, peak load, and break load locations are indicated in the upper curve as Y, P, and B respectively.**

A stress-strain curve can be obtained by dividing each load value by the initial cross-sectional area of the sample. However, the cross-sectional areas of the specimens do not remain constant during the experiment, but rather decrease. This is why here we provide load-strain curves rather than stress-strain curves.

**Table 2. Tensile test results for single layer as-r and nuc N-6 films.**

Single layer film	Width (mm)	Thickness (mm)	Yield load (N)	Break Load (N)	Break Stress (kgf/cm <sup>2</sup> )	Elongation at break (mm)	% Strain at break (%)	Energy to break (N*mm)	Young's Modulus (MPa)
as-rN6	6	0.14	24.98	54.39	666.52	136	271.9	4833.6	571.01
nucN6	6	0.11	25.06	24.55	367.14	28.7	57.5	625.99	739.4

In the low strain regions of stress-strain curves, most materials obey Hooke's law. In this region the slope of the stress-strain curve is a constant value. This constant slope equals the Young's Modulus or modulus of elasticity and this region is called the elastic region. In this region the material acts like a rubber, and completely recovers its structure when the applied load is removed [8]. Young's moduli of single layer as-r and nuc N-6 films, listed in Table 2, were determined from the slope of the curve in the elastic region by employing the tensile tester's

computer program. As seen in Table 2, single layer nuc N-6 films have a higher modulus of elasticity than single layer as-r N-6 films.

At higher strains, there is no linear proportionality between stress and strain. This nonlinearity is generally related to irreversible stress-induced plastic flow in the specimen. In the case of semi-crystalline polymers this plastic flow requires dislocation of crystalline block segments. Materials lacking this mobility, due to internal microstructures that block dislocation motion, are usually brittle rather than ductile [8]. Brittle and ductile materials differ in their stress-strain curves. Brittle materials have linear stress-strain curves over their full range of strain without noticeable plastic flow until fracture occurs. On the other hand, ductile materials have linear stress-strain curves until the yield stress and then the plastic deformation of the specimen starts. As seen in Figure 13, as-r N-6 films fracture in a ductile fashion, while nuc N-6 films shows fracture similar to brittle materials. Since nucleated films have a higher amount of crystallinity, they have limited mobility. This is why it's difficult to identify a plastic region in the load-strain curve of single layer nuc N-6 films.

The yield stress is the stress required to stimulate plastic deformation in the specimen [8]. The yield load is marked with the letter Y in Figure 13. Yield loads (N) of single layer as-r and nuc N-6 films are given in Table 2. Single layer nuc N-6 film has a slightly higher yield load, however, the average sample thickness for the nuc N-6 films is less than as-r N-6 films. This is why the yield stress of single layer nuc N-6 film is much higher than single layer as-r N-6 film.

In the case of ductile materials, a phenomenon called necking occurs right after the yield load. Until the neck forms, the deformation is mainly uniform throughout the specimen, but after

necking all subsequent deformation takes place in the neck [8]. The neck propagates until it reaches the full gage length of the specimen, a process called drawing. Interestingly, necking creates a stronger microstructure whose breaking load is greater than the yield load. This can be simply explained by increased orientation in the direction of the applied load. As a result of neck formation, single layer as-r N-6 film has a significant difference between its yield and break loads, while single layer nuc N-6 film exhibit almost the same yield and break loads (see Table 2).

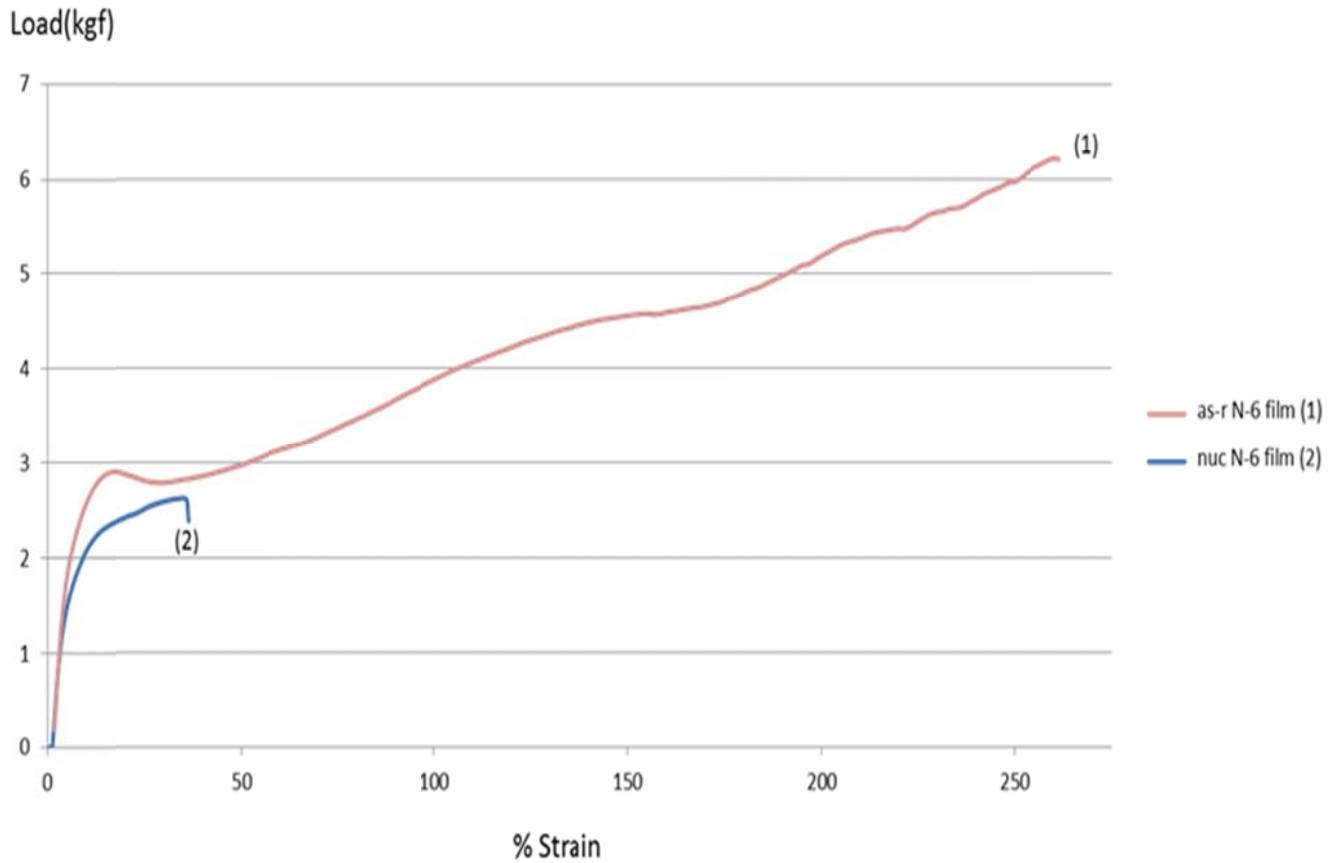


**Figure 14. Load-strain curves of single layer as-r N-6 (1) and nuc N-6 (2).**

“The total mechanical energy per unit volume consumed by the material in straining it to that value is the area under the stress-strain curve up to a given value of strain [8].” The software that we used gives the energy to break (N\*mm), which is the area under the load-elongation curve. This energy to break data corresponds to toughness, which is the area under the stress-strain curve.

There is a significant difference between the necessary energies to break the single layer as-r N-6 and nuc N-6 films, as evidenced by the load-strain responses of single layer as-r and nuc N-6 films presented in Figure 14. Note that energy to break increases quadratically with elongation or load, because it is the area under the load-elongation curve. The single layer as-r N-6 elongates 136 mm, while the nuc N-6 film elongates only 28.7 mm. This is why single layer as-r N-6 film requires almost 8 times more energy to break than the nuc N-6 film (see Table 2).

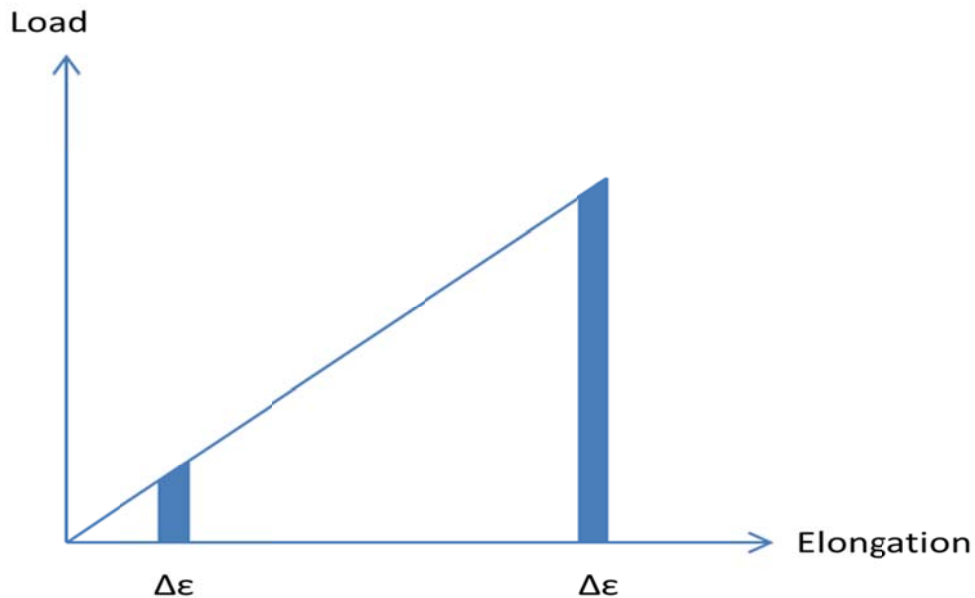


**Figure 15. Energy associated with increments of strain [8].**

In addition, Figure 15 schematically depicts the available amount of energy required to break for two equal increments of strain  $\Delta\epsilon$ , applied at different levels of existing elongation. In later elongation, the same amount of stretching requires much more energy to break the material [8]. This also increases the difference between the energy to break values between single layer as-r and nuc N-6 films. Finally it is a fact that ductile materials are generally tougher than brittle materials [8].

Tensile test results in Table 2 indicate that nucleated single layer N-6 films have lower elongation at break and higher Young's modulus than as-r N-6 films. Single layer nuc N-6 films also have greater yield stress than as-r N-6 films. These are plausible results because nucleated N-6 films have higher crystallinity than as-r N-6 films. It is a fact that crystalline regions act like large cross-links and decreases elongation and increases modulus and strength.

**Table 3. Crystallinity values of as-r, nuc, and annealed N-6 single layer films.**

Single Layer Film	$\Delta H_m$ (J/g)	% Crystallinity *
as-r N-6	58.8	36
nuc N-6	83.4	52
Annealed N-6	84	52

\*%Crystallinity values were calculated by Equation 1.

In order to eliminate the effect of crystallinity and see that if nuc N-6 film has superior mechanical properties to use as reinforcing unit, we annealed the as-r N-6 films at 180 °C for 27 hours and obtained the same amount of crystallinity as the nuc N-6 films. The melting endotherms of as-r, nuc, and annealed N-6 and their % crystallinity values are listed in Table 3.

After obtaining the same amount of crystallinities for annealed and nuc N-6 films, tensile tests were conducted for annealed films. As seen in Figure 16, nucleated films have higher modulus and lower % elongation at break than annealed films. These results clearly show that nucleated films can be used as the reinforcing unit, because they have superior properties to as-r N-6 and even to annealed as-r N-6 films.

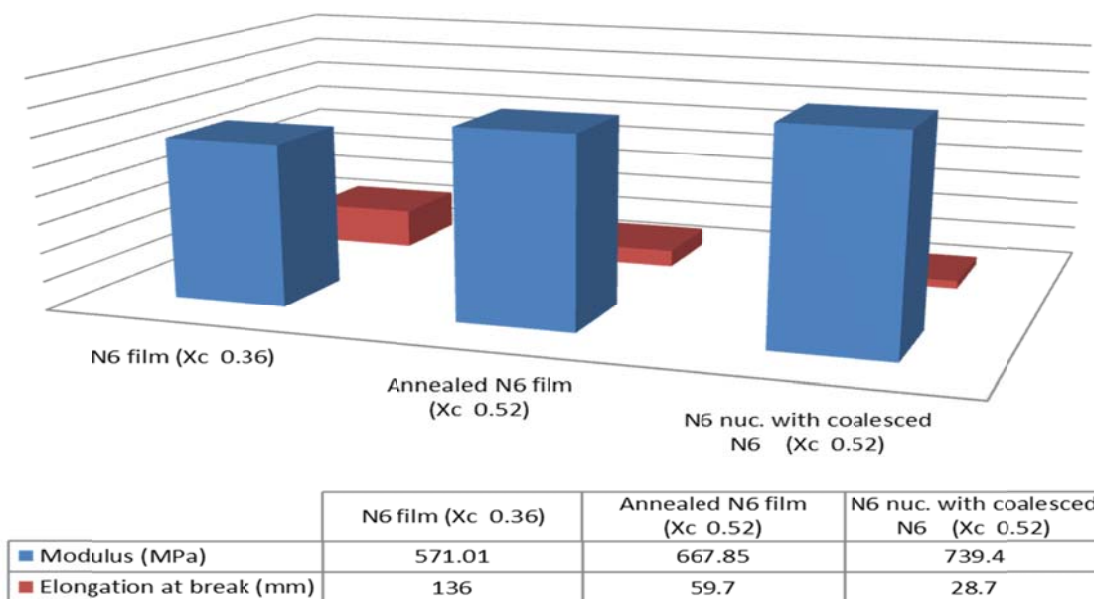


**Figure 16. Stress-strain responses of thin melt-pressed neat bulk N-6 films (as-received and annealed), and N-6 film nucleated with N-6 coalesced from its 1:1 stoichiometric  $\alpha$ -CD-IC**

[5].

In Figure 16 we can see that the N-6 film nucleated with 2 wt% of N-6 coalesced from its stoichiometric 1:1  $\alpha$ -CD-IC has a higher modulus and a greatly reduced elongation at break compared to the neat N-6 films, even after annealing to achieve a closely similar level of crystallinity as the nucleated N-6 film. We believe this to be a consequence of the more homogeneous and finer scale semi-crystalline morphology and possibly the increased packing density of un-entangled and extended N-6 chains in the non-crystalline regions [4, 5].

### 3.3.5. Characterization of Single-Component as-r and nuc Nylon 6 Composites

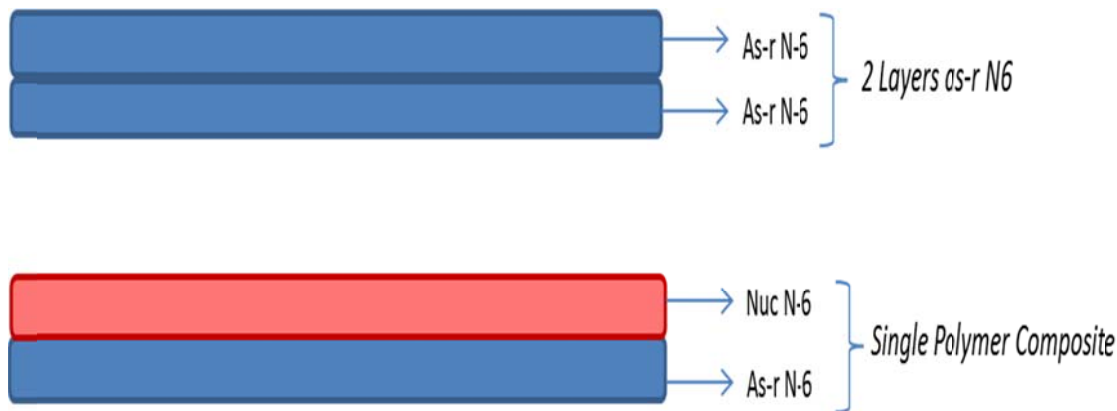


**Figure 17. Schematic representation of two layer as-r N-6 sandwich, and Single Component as-r N-6/nuc N-6 Composite.**

Thus far, we have shown that coalesced N-6 has properties distinct from as-r N-6 and can, when used in small amounts, serve as an effective nucleating agent. When we made melt pressed films of nucleated N-6, we found that they have higher modulus and lower elongation at break. By using nuc N-6 film as the reinforcing unit, and as-r N-6 film as matrix, we will make self-reinforcing, single-component polymer composites. This self-reinforced N-6 composite will be

made by melt-pressing nuc N-6 film onto as-r N-6 film. Finally we will compare the properties of our composite with two layers of as-r N-6. A schematic representation of such two layers sandwich films are given in Figure 17.

According to the definition of a composite, which we discussed and adopted in chapter 2, a composite is a “multiphase material formed from a combination of materials which differ in composition or form, remain bonded together, and retain their identities and properties”. From this definition, there are three main characteristics that a composite has to have, and they are,

- 1-There has to be two distinct materials,
- 2-These two different materials have to stay together,
- 3- They should retain their distinct characteristic behaviors.

In order to state that we have a composite, our single-component self-reinforced composite has to demonstrate these characteristics. Our discussion shows that as-received and nucleated N-6 are two different forms of the same polymer. They have different crystallinities,  $T_c$ 's, and mechanical properties, and so satisfy the first characteristic. Since these two materials have the same chemical composition, they should not have any compatibility problems, leading to a solution of the poor interface problem. The third condition is the key point for our study. In order to claim that we have a composite, these two materials have to retain their distinct properties after melt pressing the films into a sandwich. If they become a single phase material, we cannot claim this product is a composite, because it does not meet the third criterion.

The distinctive properties of the chemically identical as-r and nuc N-6 are their  $T_c$ 's and semi-crystalline morphologies. If melt-pressing these films into a two-layer sandwich yield a single  $T_c$ , this means that they have become a single phase material, not a composite.

Two types of films were made by the following method. 1 g of as-received film was melt-pressed onto 1 g of either as-received film (2 Layers of as-r N-6) or 1 g of self-nucleated N-6 film (as-rec/nuc N-6 composite) under a pressure of 2.62 MPa for 1 minute at 240 °C.

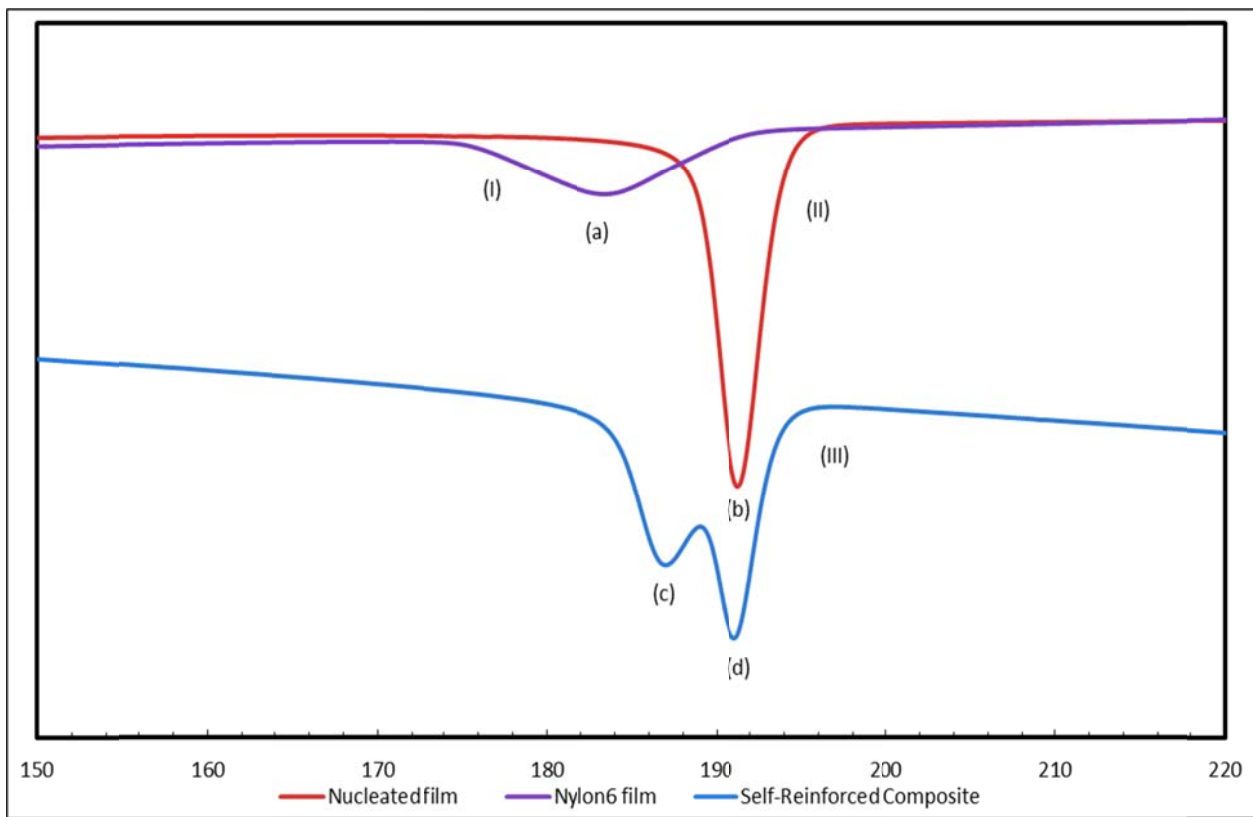


**Figure 18. DSC cooling scans from the melts of (I) as-received, (II) nucleated, and (III) asr/nuc sandwich films.  $T_c$  values are (a) 183.5, (b) 191.5, (c) 186, and (d) 191.5 °C.**

When we conducted DSC observation on the two films, we observed two distinct  $T_c$ 's for as-r N-6 and nuc N-6 films as seen in Figure 18. As we mentioned earlier,  $T_c$  of as-r N-6 film is 183.5 °C and  $T_c$  of nuc N-6 film is 191.5 °C. After melt pressing these two films under an applied pressure of 3.5 MPa, we observe two  $T_c$ 's at 186 and 191.5 °C. Clearly the exotherm at 191.5 °C is the  $T_c$  of the nucleated layer in the composite film sandwich. According to Figure 18, there is an increase in the  $T_c$  of as-r N-6. This might be either a surface/interface nucleation effect, or the effect of processing. When we melt-pressed two layers of as-r N-6 under an applied pressure of 2.62 MPa for 1 minute and afterwards conducted DSC, we found that this material also had a  $T_c$  at 186 °C. This proves that processing is causing the additional increase in  $T_c$  of the as-r N-6 sandwich layer. The DSC observations in Figure 18 clearly demonstrate that we have a composite, because after melting these two components, they retain their characteristic behaviors and did not become a single phase material.

Figure 19 presents modulus (MPa) and elongation at break (mm) values for the 2 layer as-r/as-r N-6 sandwich, and the single-component polymer composite made of one layer of as-r N-6 and one layer of nuc N-6. We can conclude from Figure 19 that the asr/nuc N-6 film sandwich has improved properties, with an increased Young's modulus (+14%) and reduced elongation at break (-92%) compared with the asr/asr N-6 sandwich film.

This single polymer composite does not have a weak interface because the two materials are highly compatible, and as seen in Figure 20, breaking occurs in both layers at the same time. Delamination occurs when the shear stress, created by an applied load, is higher than the adhesion force between the two layers. As seen in Figure 20, we did not observe delamination.

A SEM image of the cross-section of an as-r/nuc N-6 film sandwich is presented in Figure 21. This image shows the interface between two layers and it is consistent with our DSC results in Figure 18. The as-received N-6 film and the film made from N-6 nucleated with coalesced N-6 do not become homogeneously mixed after melt-pressing at 240 °C for ~5 minutes and spending an additional 5 minutes in the melt during DSC observation. Also this image shows the perfect compaction of two layers and explains why we do not observe delamination.

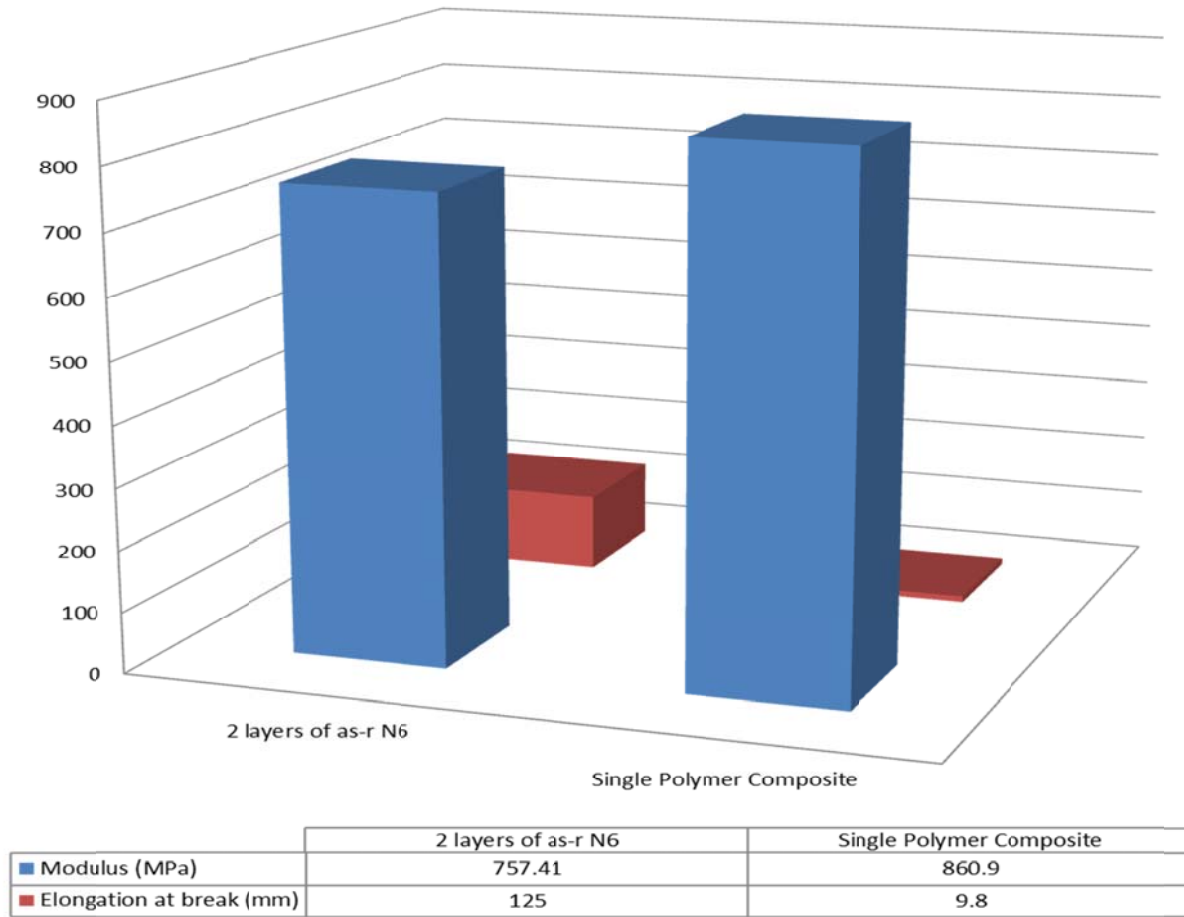


**Figure 19. Tensile tests results for asr/asr and asr/nuc N-6 sandwich films.**

From this observation we can infer that interfacial forces also prevent the elongation of the inherently more extensible as-received layer. This strong interface is the result of both component films melting during their pressing into a sandwich. Apparently spending ~10 minutes above their melting temperature provides sufficient mobility to the N-6 chains in both film layers to partially interpenetrate each other, but not to diffuse entirely through each layer. Otherwise, we could not observe two distinct DSC behaviors as seen in Figure 18.

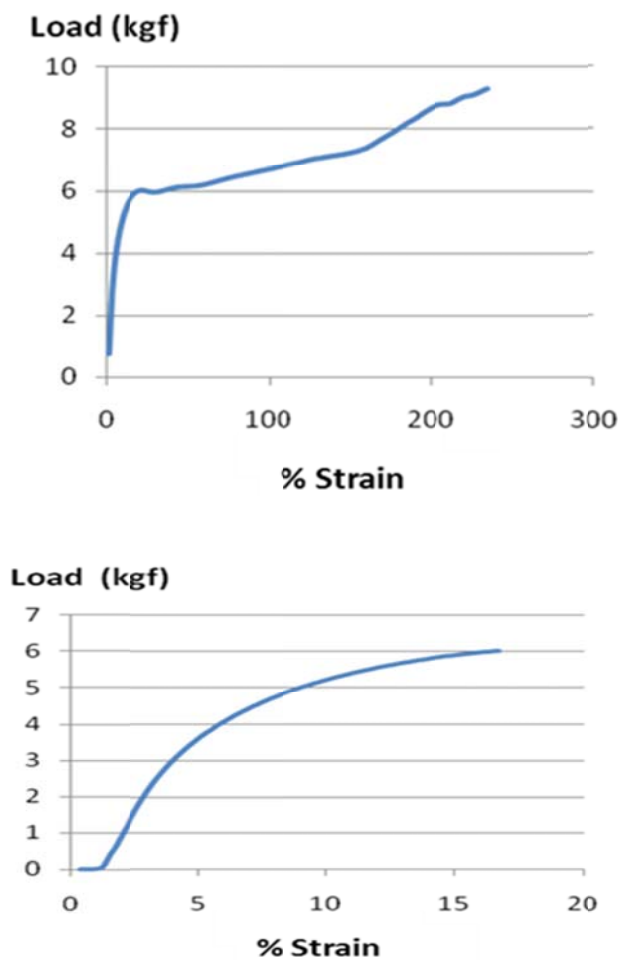


**Figure 20. Response of asr/asr (upper) and asr/nuc (lower) N-6 sandwich films to applied load.**

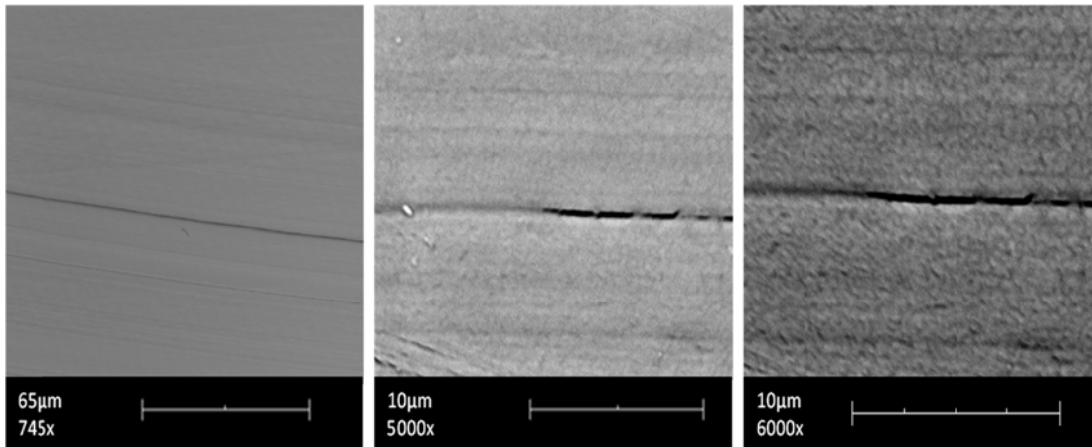


**Figure 21. SEM images of the cross section of single-component as-r/nul-N-6 composite.**

### **3.4. Conclusions**

In this work, we introduced a novel method to produce single-component polymer composites. The reinforcement and the matrix components of the composite are composed of chemically identical, but morphologically distinct, forms of the same polymer, Nylon-6 (N-6).

A N-6 sample morphology different from the as-received polymer was obtained by processing each individual polymer chain with  $\alpha$ -cyclodextrins ( $\alpha$ -CD). N-6 chains were completely covered with  $\alpha$ -CDs, forming a stoichiometric inclusion compound (IC), 1:1 N-6  $\alpha$ -CD-IC. Subsequently, the host  $\alpha$ -CD channels were removed by washing the IC with excess deionized water. This coalescence process yields extended and untangled chains, a finer-scale semi-crystalline morphology, higher amounts of crystallinity, higher melt-crystallization temperatures,  $\alpha$ -crystalline morphology in the crystalline regions, and higher density and orientation in non-crystalline regions. All of these distinct behaviors serve to improve the mechanical properties of N-6 films that were self-nucleated by adding 2 wt% of coalesced N-6.

Tensile tests showed that single layer nuc N-6 films have higher Young's modulus and lower elongation than single layer as-r N-6 films. This is why we used single layer nuc N-6 film as the reinforcement component in our prototype composite and an as-r N-6 film as matrix. As discussed in a previous section, DSC results in Figure 18 prove that our single-component N-6 film sandwich composite does not become a homogeneous single phase material after melt-processing for at least 10 min. Our SEM images and the load-strain curves both indicate a strong interface between the inherently compatible layers. The single-component as-r/nuc N-6 composite has a higher modulus of elasticity and lower % strain at break than an as-r/as-r N-6 film sandwich.

Finally, single-component polymer composites were produced that exhibited higher Young's modulus, lower elongation, and extremely strong interfaces. Single-component polymer composites should be generally expected to eliminate the problems caused by weak interfaces between the reinforcement and matrix, and will certainly simplify their recycling.

## REFERENCES

1. Gong Y, Yang G. Single polymer composites by partially melting recycled polyamide 6 fibers: Preparation and characterization. *Journal of Applied Polymer Science*, 118: 3357–3363. doi: 10.1002/app.3236. 2010.
2. Tonelli AE. Molecular Processing of Polymers with Cyclodextrins, *Adv Polym Sci*, 222: 115–173. 2009.
3. Wei M, Davis W, Urban B, Song Y, Porbeni FE, Wang X, White JL, Balik CM, Rusa CC, Fox J, Tonelli AE. Manipulation of Nylon-6 Crystal Structures with Its  $\alpha$ -Cyclodextrin Inclusion Complex, *Macromolecules*, 35, 8039. 2002.
4. Mohan A, Joyner X, Kotek R, Tonelli AE. The Constrained/Directed Crystallization of Nylon-6: I. Non-stoichiometric Inclusion Compounds formed with Cyclodextrins, *Macromolecules*, 42, 8983-91. 2009.
5. Mohan A, Gurarslan A, Joyner X, Child R, Tonelli AE. Melt-Crystallized Nylon-6 Nucleated by the Constrained Chains of Its Non-Stoichiometric Cyclodextrin Inclusion Compounds and the Nylon-6 Coalesced from Them, *Polymer*. 2010. doi: 10.1016/j.polymer.2010.12.049
6. Mohan A. Modification of Nylon 6 Structure via Inclusion. PhD Thesis. North Carolina State University. 2009.
7. Fornes TD, Paul RD, Crystallization Behavior of Nylon 6 Nanocomposites, *Polymer*, 44: 3945-3961. 2003.

8. David Roylance, "Stress-Strain Curves," Department of Materials Science and Engineering, Massachusetts Institute of Technology, (2001) <http://www.myoops.org/twocw/mit/NR/rdonlyres/Materials-Science-and-Engineering/3-11Mechanics-of-MaterialsFall1999/1B957032-BE5D-4475-8CDE-6D29E9EB6502/0/ss.pdf>.
9. Bullions TA, Wei M, Porbeni FE, Gerber MJ, Peet J, Balik CM, Tonelli AE. Reorganization of the Structures and Morphologies of Bulk Polymers via Coalescence from their Polymer Cyclodextrin Inclusion Compounds, *J. Polym. Sci., Polym. Phys. Ed.*, 40, 992. 2002.
10. Williamson BR. Processing Polymers with Cyclodextrins. PhD Thesis. North Carolina State University. 2010.

# CHAPTER 4

## Future Work

### 4.1. Future Studies

The aim of this study was to determine whether a single-component polymer composite might be produced by using chemically identical as-received and cyclodextrin processed polymer samples. Results presented in this thesis prove that it is possible to make a single-component polymer composite from polymers that are chemically identical, but that have different semi-crystalline morphologies.

Future studies can examine processing details, such as how much time is required for the composite sandwich of as-r N-6/nuc N-6 layers to become homogeneous in structure and behavior during melt-processing? Also multi-layer laminates, such as as-r/nuc/as-r and nuc/as-r/nuc N-6 “triple-decker” film sandwiches can be produced and their mechanical properties examined.

Because we observed that the as-r N-6/nuc N-6 sandwich did not become a single-phase material during ~10min of melt-processing, we can attempt to produce nuc N-6 fibers. Nuc N-6 fibers can then be embedded in an as-r N-6 matrix to produce a fiber-reinforced single-component composite. Bi-component fibers with self-nucleated cores and as-received sheaths could also be produced. In addition, the hot compaction method might be attempted with fabrics woven with both nuc and as-r N-6 yarns.

Self-nucleating agents can also be produced by coalescing polymers, such as poly( $\epsilon$ -caprolactone) (PCL), poly(L-lactic acid) (PLLA), poly(ethylene terephthalate) (PET), etc., from their CD-ICs [2]. PCL and PLLA are both bioabsorbable and biodegradable polymers used in implantable textile and other devices. Their single-component composites might offer a viable way to improve their performance without introducing any other chemicals.

As a final example, single-component PET composites might be used to manufacture bottles with improved strengths and barrier properties, without using additional materials that would complicate their recycling.